A Method for Automated Landmark Constellation Detection Using Evolutionary Principal Components and Statistical Shape Models

Wei Lu MS Thesis Defense
Supervisor: Dr. Hans J Johnson
Friday, November 19, 2010
2:00 – 4:00 PM, 4016 Seamans Center

Motivations for automation

- Good news: current imaging technology provides ☺
  - Images with improved spatial resolution
  - High volumes of data
  - Research studies commonly have with hundreds of scans
- Bad news: there is a lot of data ☹
  - Require increased data processing time
- Therefore: we need automated tools

Motivations – Golden Standard

- Human placement of landmark points (widely used):
  - Labor-intensive (expensive)
  - Subjective
  - Intra/inter-rater inconsistent
  - Not scalable
    - Hard to hire
    - Hard to train
    - Hard to keep busy all the time /
      or it takes a long time to complete the work

Motivations – Desired Properties

- Computer-aided detection method:
  - Automated (little human efforts required)
  - Efficient (vs. human labeling)
  - Consistent (reproducible)
  - Accurate (similar to human)
  - Generalizable
    - Different modalities
    - Different anatomical regions
  - Robust
    - Noise
    - Orientation
    - Spacing
    - Origin

Method Overview

Top level data flow diagram

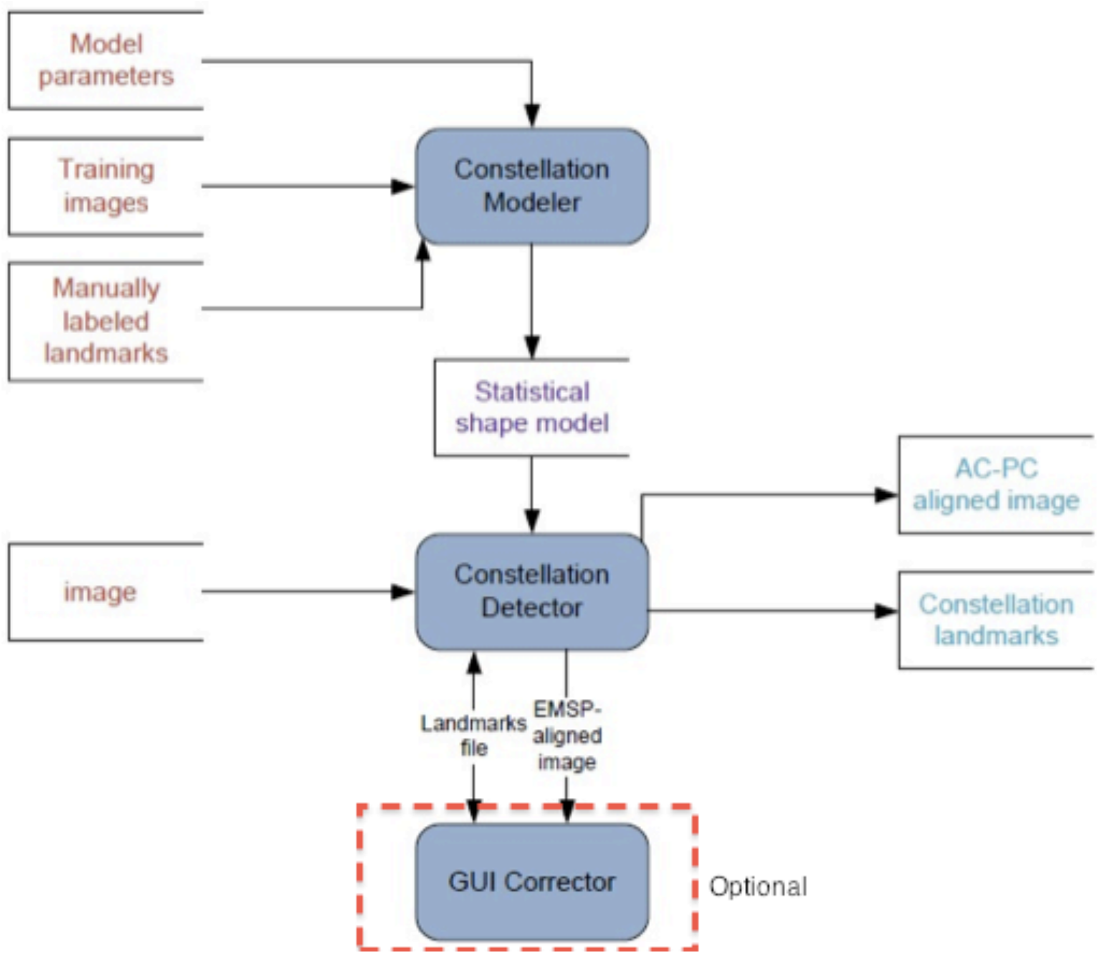

The University of Iowa College of Engineering

Constellation GUI corrector

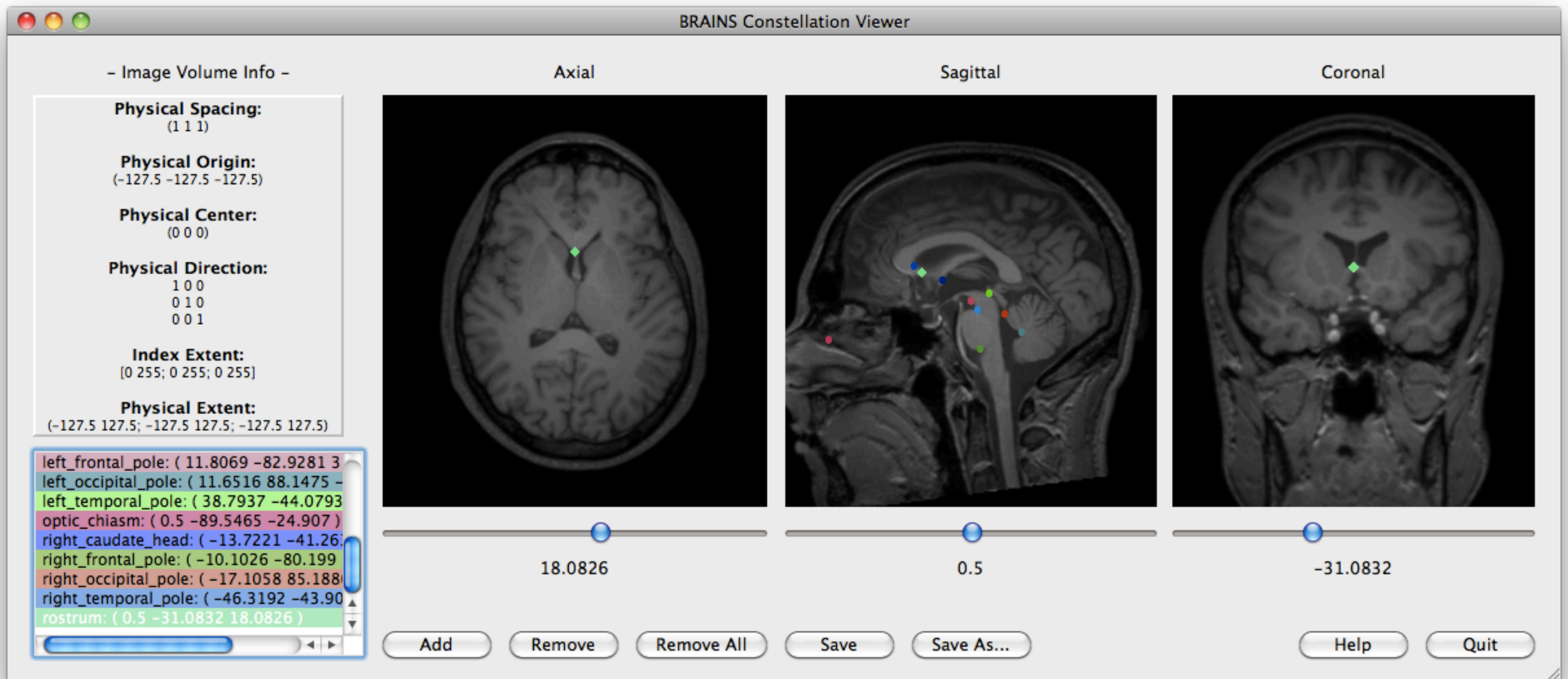

Processing Phases

- Landmarks are estimated in a simple to hard, special to general fashion.
- First: find a few reference points/planes
  - Centroid of head mass
  - Mid-sagittal plane transform
  - Eye centers
- Second: most landmarks will be found by a linear model estimation method.

Centroid of head mass estimation

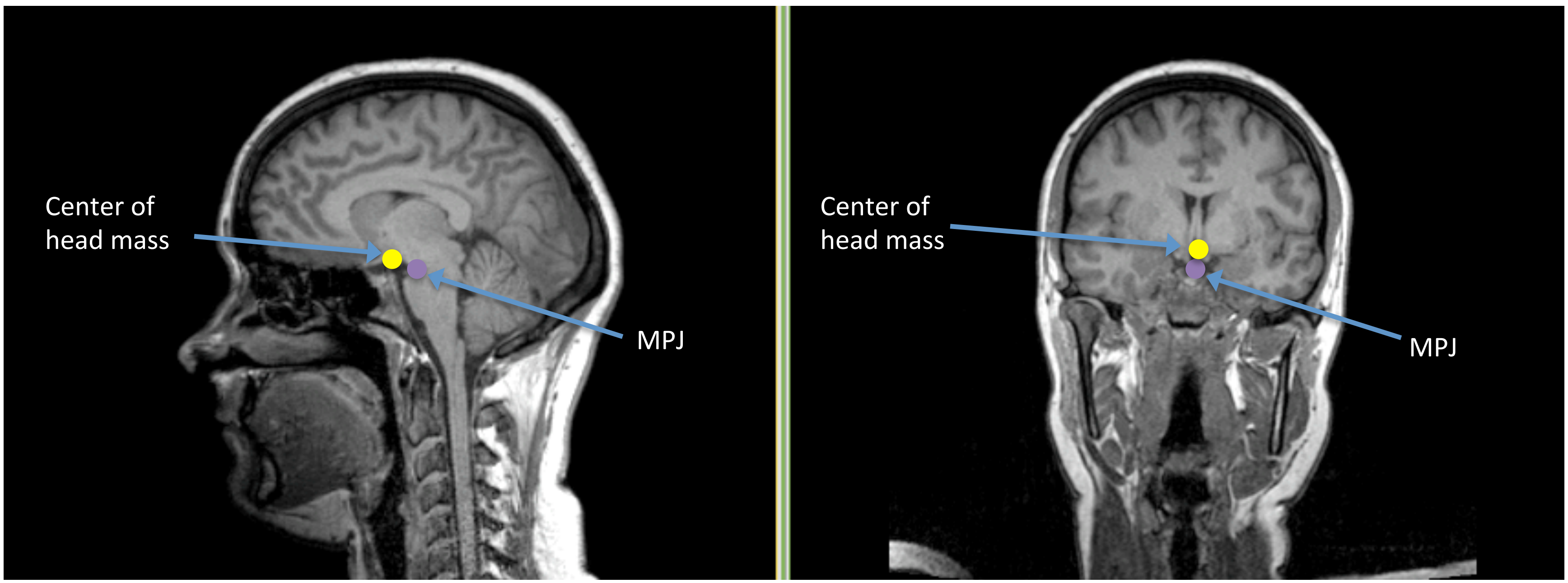

1. CoHM is processed first as it can be estimated independently.
2. The spatial location is usually stable and very close to the MPJ.

Centroid of head mass estimation

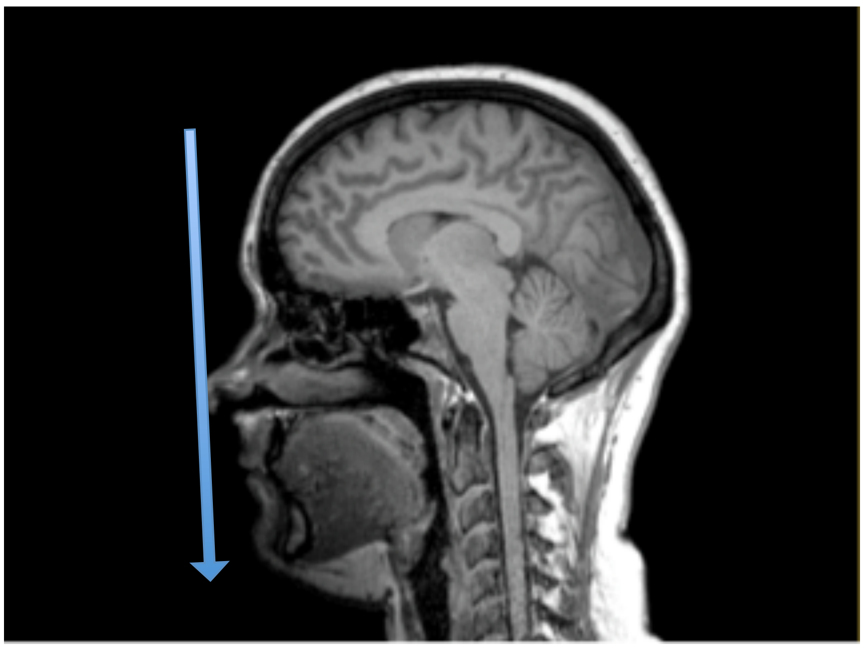

Centroid of head mass estimation

Centroid of head mass estimation

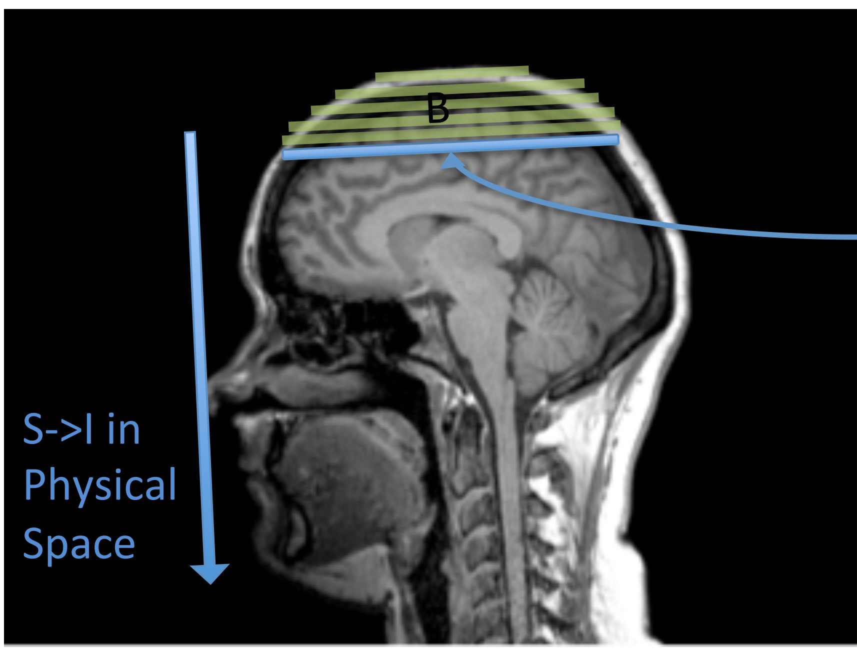

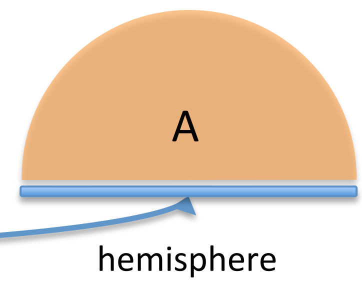

B_i: foreground object slice in *i*th iteration

$B_{max\text{-}so\text{-}far} = \max(B_i),\ i = 1, 2, \ldots, curr$
$r = \mathrm{sqrt}(B_{max\text{-}so\text{-}far}/\pi)$
$V_A = ½ \times 4/3\pi r^3$
$V_B = \mathrm{sum}_{i=1:curr}(B_i \times \mathrm{thickness})$
Thickness = 3 *mm*

Stop criteria: Until $V_B > V_A$

Centroid of head mass estimation

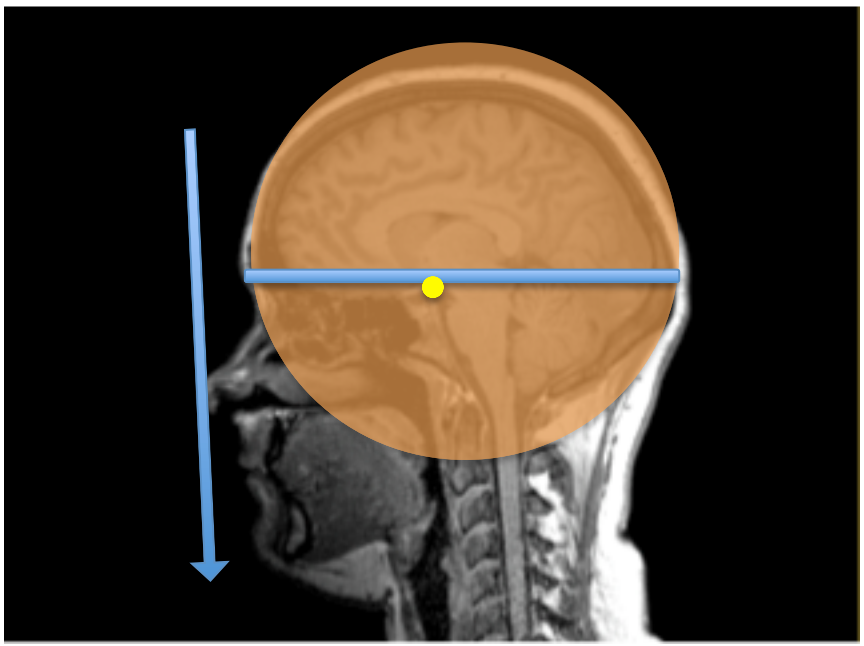

Centroid of head mass estimation

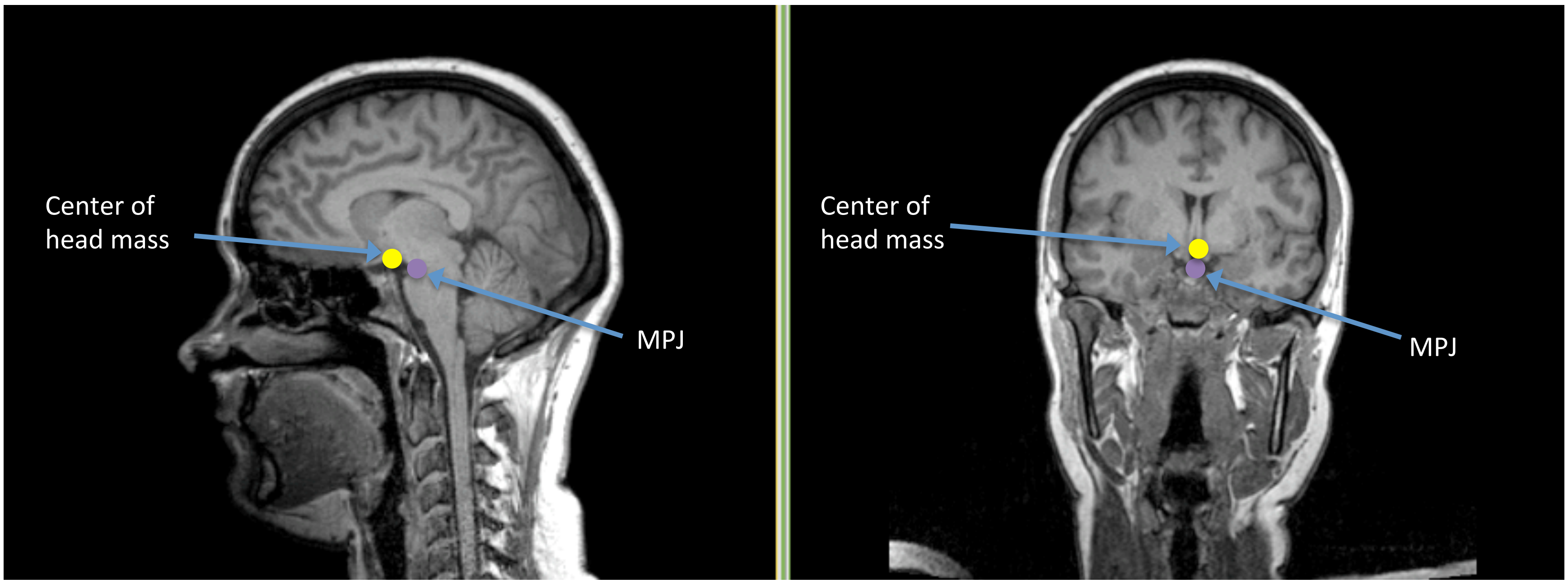

Centroid of head mass estimation

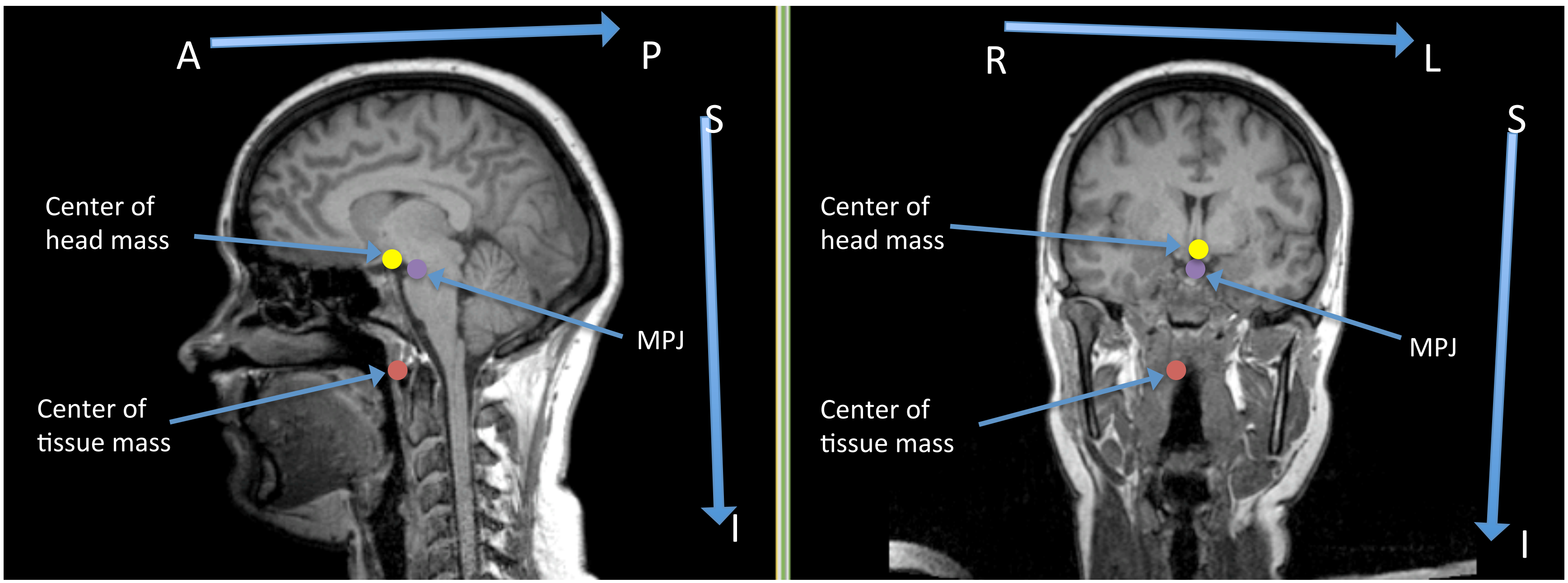

Compared to center of mass, CoHM is more robust to input image with lots of neck and shoulder portion. That is, CoHM is still very close to MPJ as is expected.

Mid-sagittal plane transform estimation

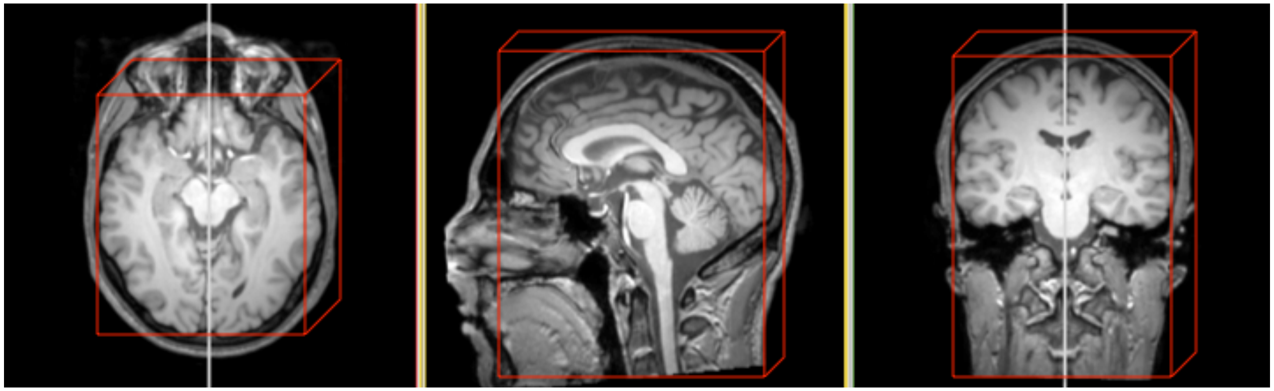

(a)

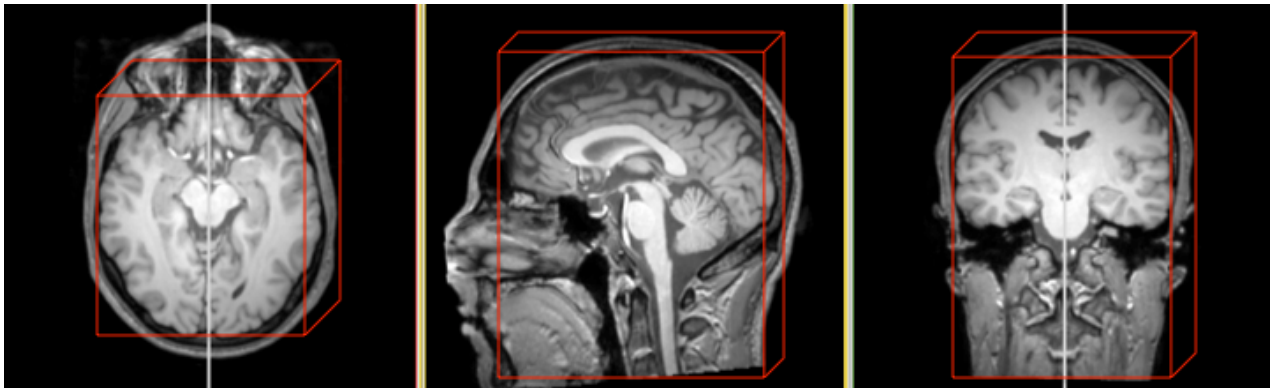

(b)

3D -> 2D, good for base landmark detection

Mid-sagittal plane transform estimation

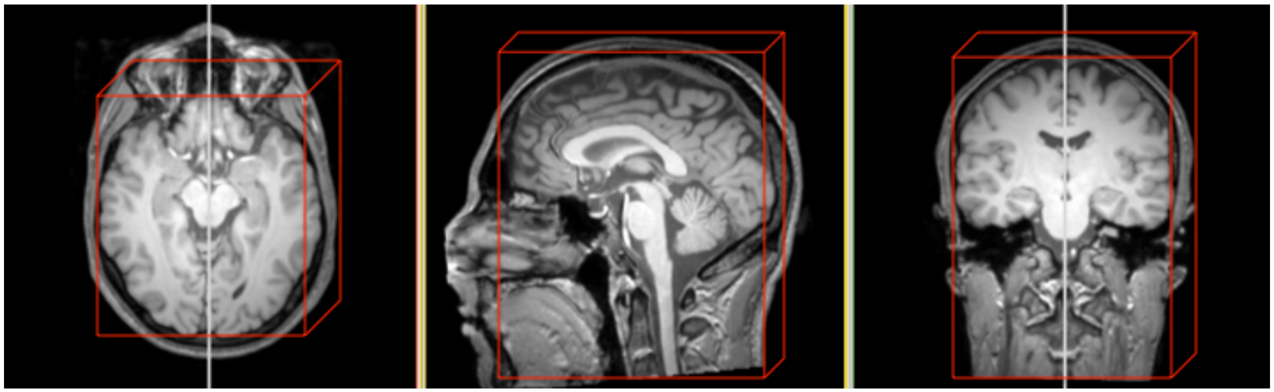

(a)

(b)

Optimal transform: Maximize the reflective correlation in the bounding box centered at CM using Powell's optimizer

Mid-sagittal plane transform estimation

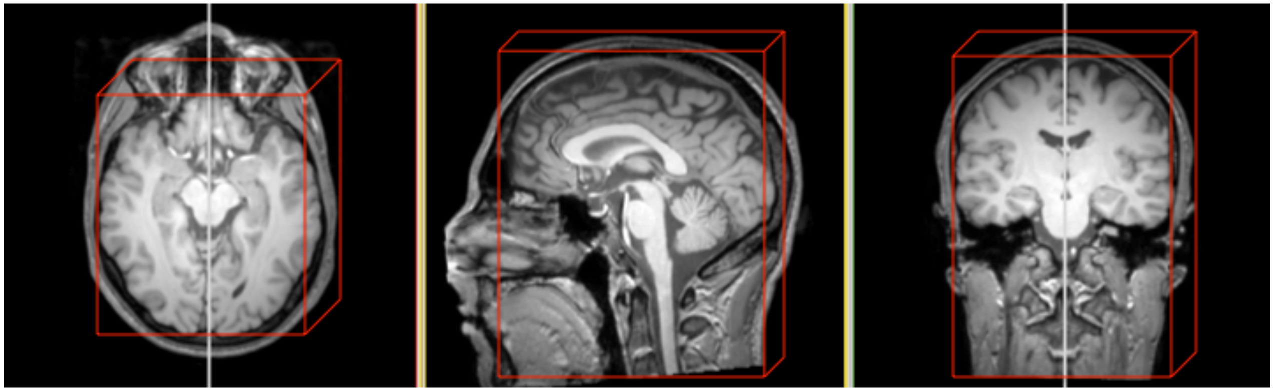

(a)

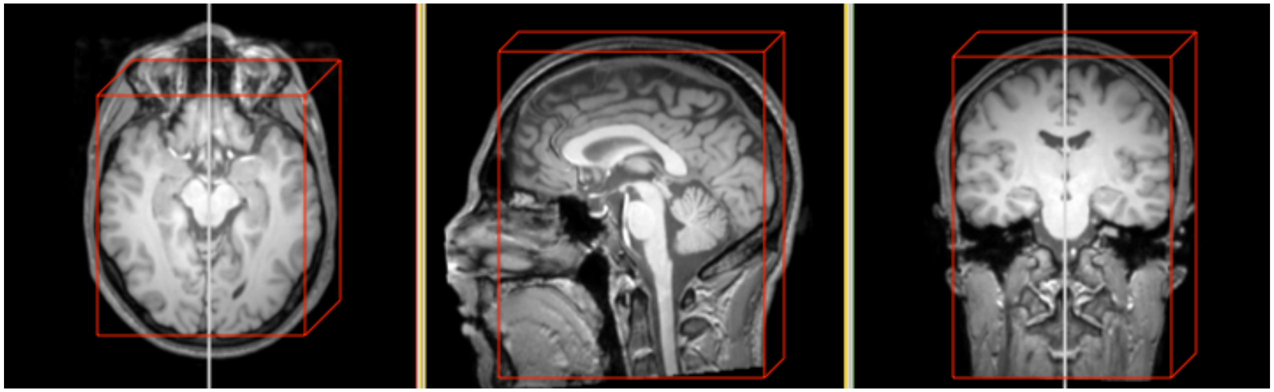

(b)

Reflective correlation: Correlation of the intensities of reflected pixels about the MSP and inside the bounding box

Sphere detection using radial Hough transform

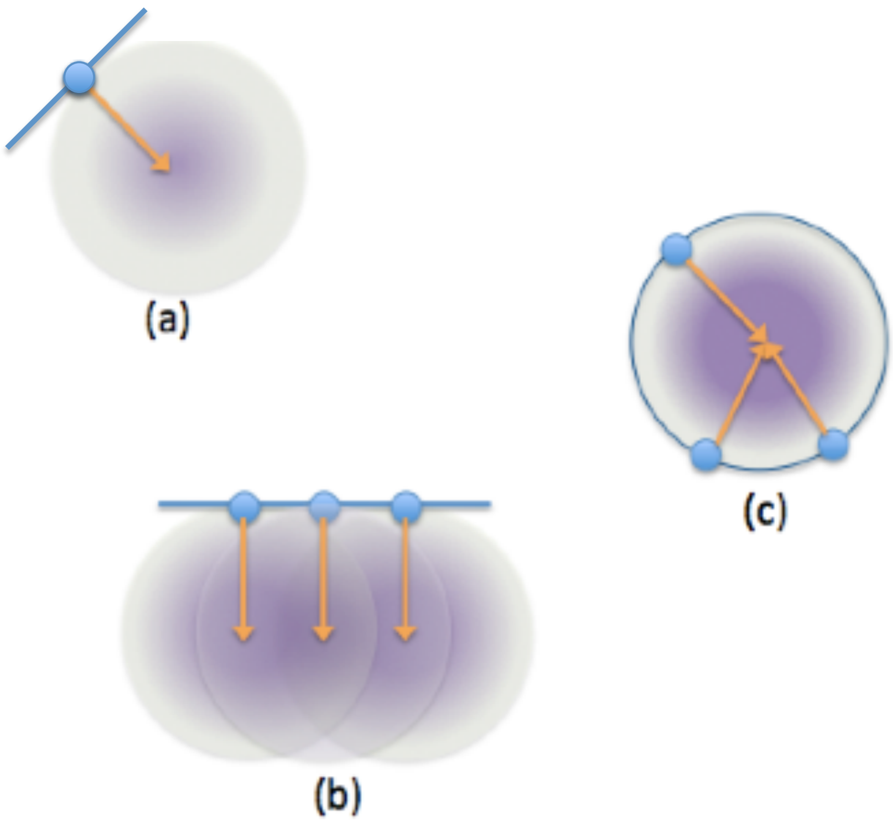

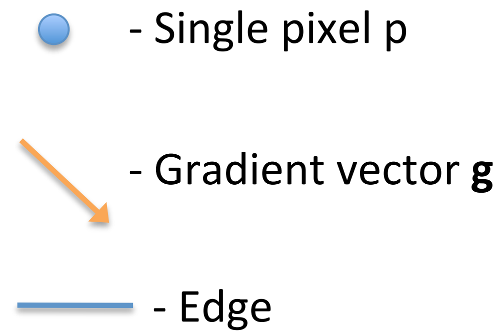

g(p) = (∂f(x,y)/∂x, ∂f(x,y)/∂y) | (x,y) = p

An 2D illustration showing sphere detection using radial Hough transform

Eye detection using radial Hough transform

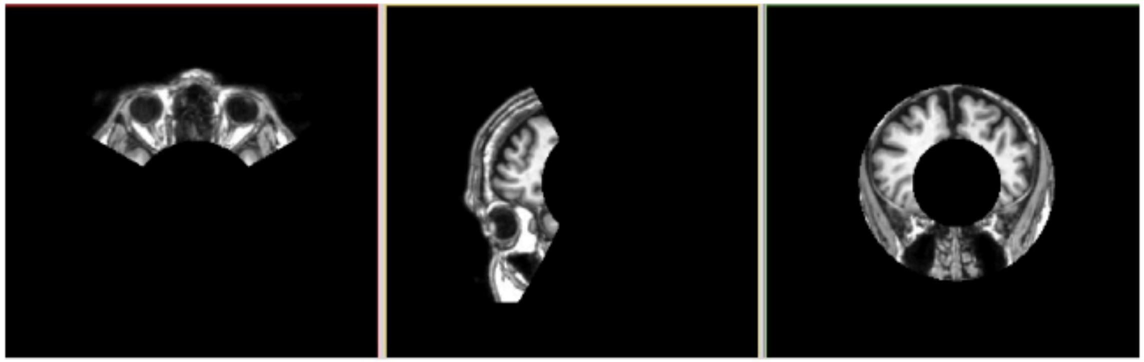

(a) A typical ROI image for eye centers in (a) axial view, (b) sagittal view, and (c) coronal view

(b) A typical accumulator image for eye centers in (a) axial view, (b) sagittal view, and (c) coronal view

Eye detection demo

Diameter of eyes: 24 *mm* [1]

[1] Britannica Inc. Encyclopedia Britannica Macropedia: Sensory Reception. Britannica Inc., USA, 1997

THE UNIVERSITY OF IOWA
College of Engineering

Eye detection using radial Hough transform

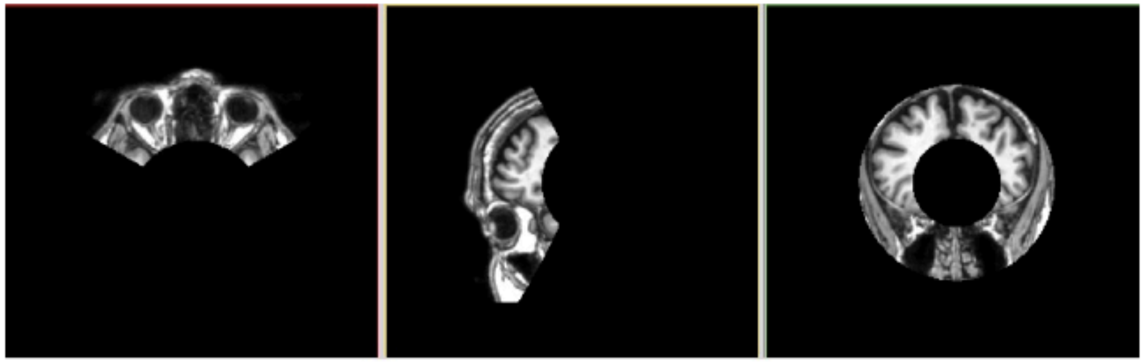

(a) A typical ROI image for eye centers in (a) axial view, (b) sagittal view, and (c) coronal view

(b) A typical accumulator image for eye centers in (a) axial view, (b) sagittal view, and (c) coronal view

Eye detection demo

ROI: truncated spherical sector

R_1 = 120 *mm,* R_2 = 30 *mm,* Spread angle = 2.4 *rad*

The University of Iowa
College of Engineering

Verification for Eye detection

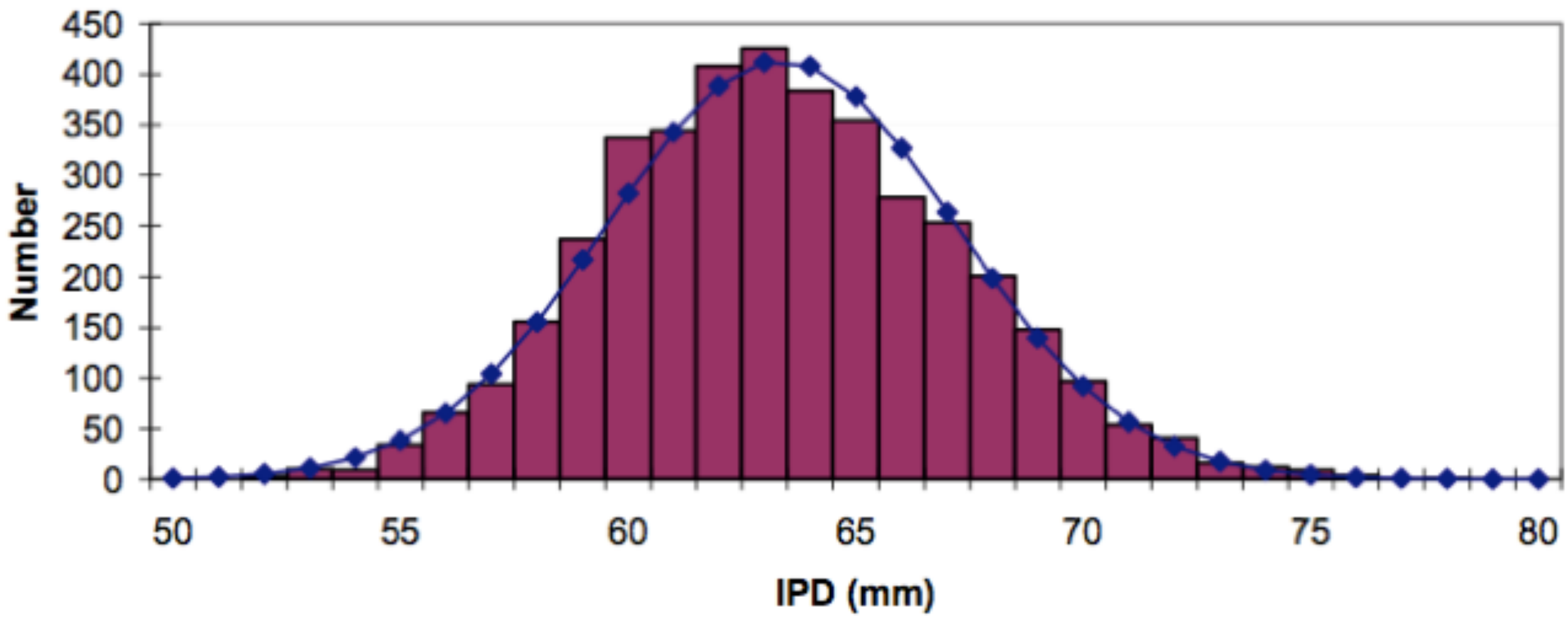

Distribution of IPD for the entire ANSUR database [1]

[1] Figure courtesy of Neil A. Dodgson, Proc. SPIE Vol. 5291

Eye detection using radial Hough transform

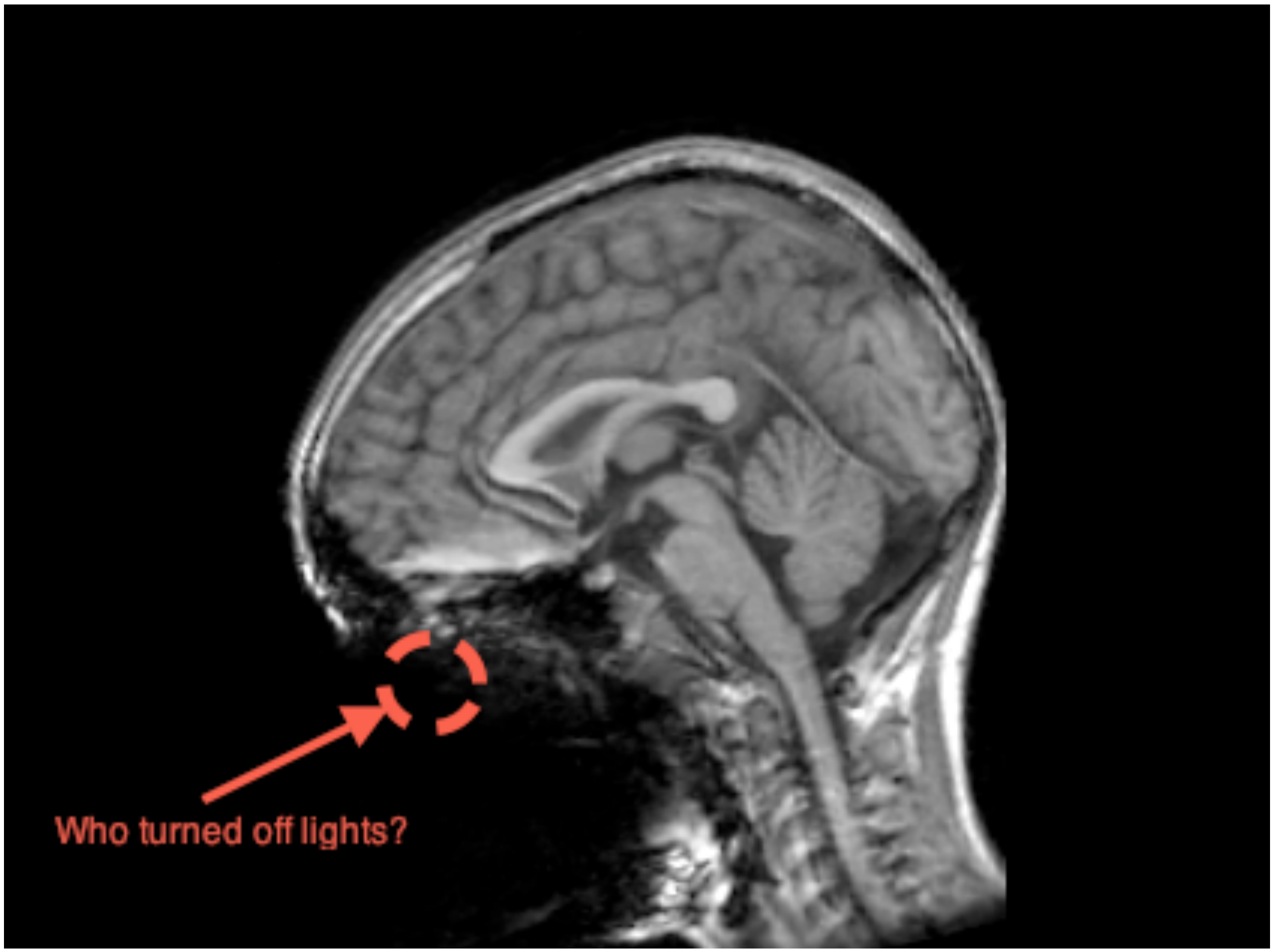

Eye detection failure case

Linear model prediction

Morphometric constraining

1. Human brains share a similar angle from $\overrightarrow{CEC} - \overrightarrow{MPJ}$ to $\overrightarrow{4VN} - \overrightarrow{MPJ}$
2. Human brains share a similar angle from $\overrightarrow{CEC} - \overrightarrow{MPJ}$ to $\overrightarrow{ac} - \overrightarrow{MPJ}$
3. Human brains share a similar $||\overrightarrow{4VN} - \overrightarrow{MPJ}||$
4. Human brains share a similar $||\overrightarrow{ac} - \overrightarrow{MPJ}||$
5. *4VN* is always below the $\overrightarrow{MPJ} - \overrightarrow{CEC}$ line on the *EMSP* plane
6. *ac* is always above the $\overrightarrow{MPJ}$ - $\overrightarrow{CEC}$ line on the *EMSP* plane
7. The *CEC*, *MPJ*, *4VN*, *ac* and *pc* are all very close to the *EMSP* plane
8. Nearby landmarks share a linear relationship in location

Morphometric constraining

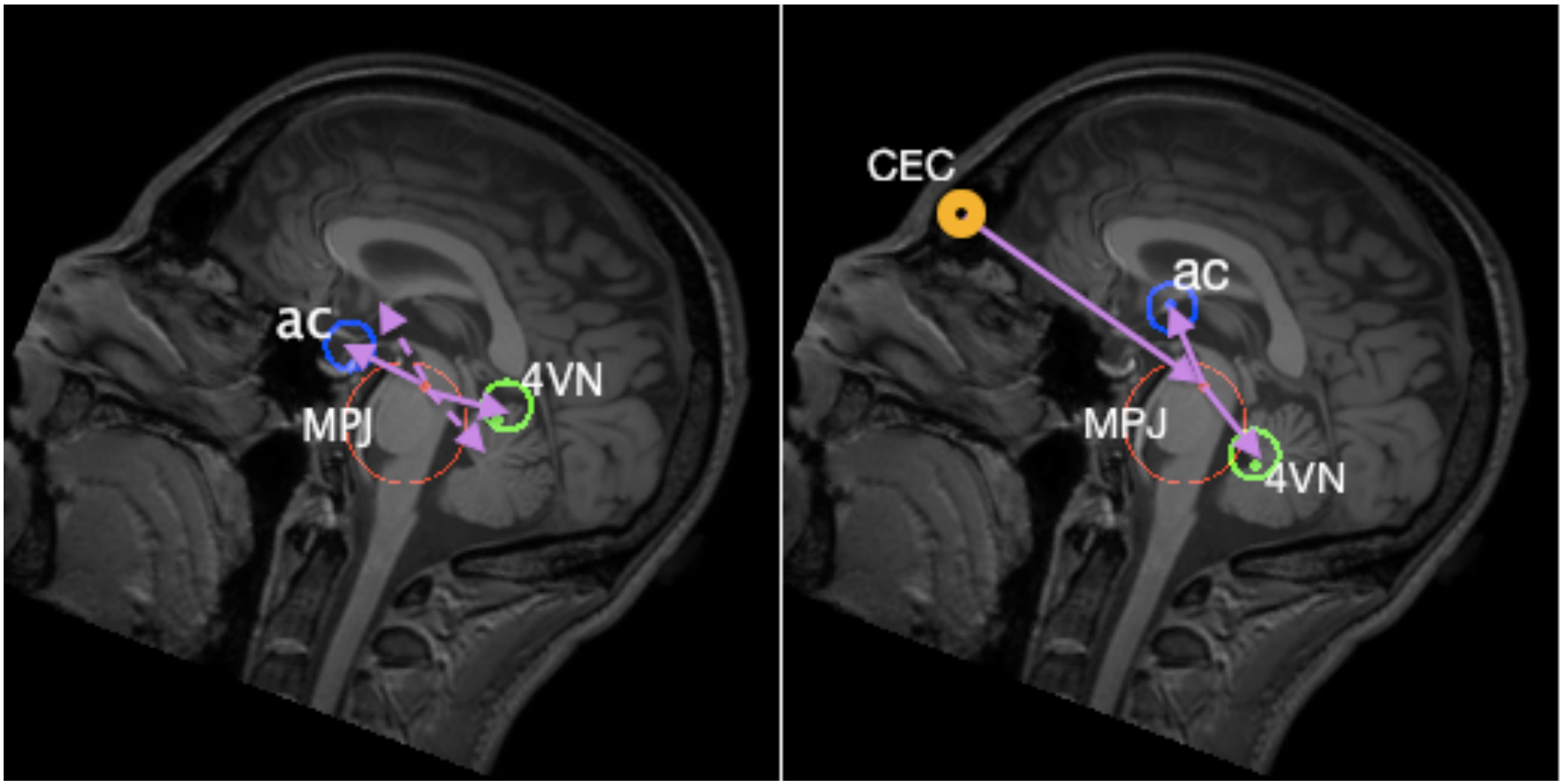

The information of CEC improves the robustness for ac and 4VN detection

Linear model estimation using Evolutionary PCA

- The relationship between each new landmark is trained by a linear combination of its principal components extracted from the landmarks appearing before it in the processing list.
- New landmarks are estimated one by one, evolutionarily taking the advantage of knowing more information.
- Exploit PCA to extract the most efficient basis to represent a new landmark vector. (scalable)

EPCA demo

Physical vector space

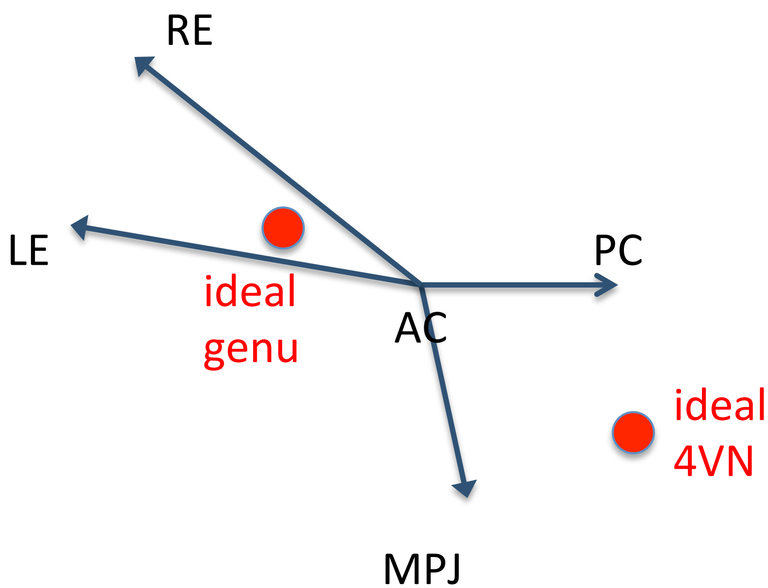

Precondition: Some of the landmarks (e.g. LE, RE, AC, PC, and MPJ) have been estimated well in physical space.

Postcondition: Locations of a list of new landmarks (e.g. 4VN, genu, etc.) are estimated reasonably.

EPCA demo

Principal component space

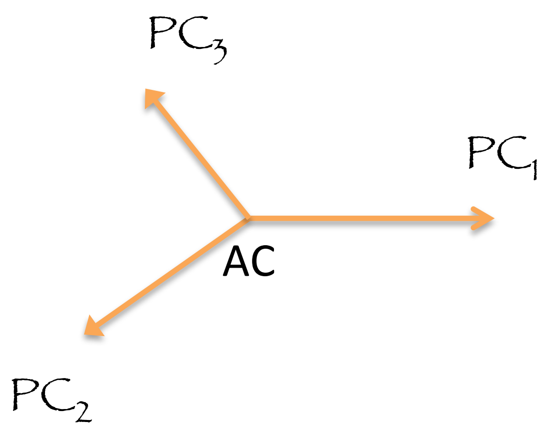

All the landmark vectors are transformed into their principal component space.

$$Z = W^T X$$
$$W_{opt} = [w_1, w_2, \ldots, w_r]$$
$$w_i := eig(cov(X), i),$$
$$\forall i \in \{1, 2, \ldots, r\}$$

EPCA demo

Principal component space

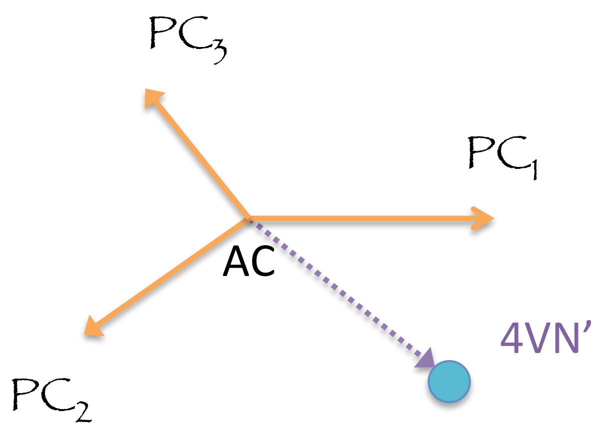

New landmark (e.g. 4VN) location is estimated by its morphometric relationship among current PCs we obtained in the training phase.

EPCA demo

Principal component space

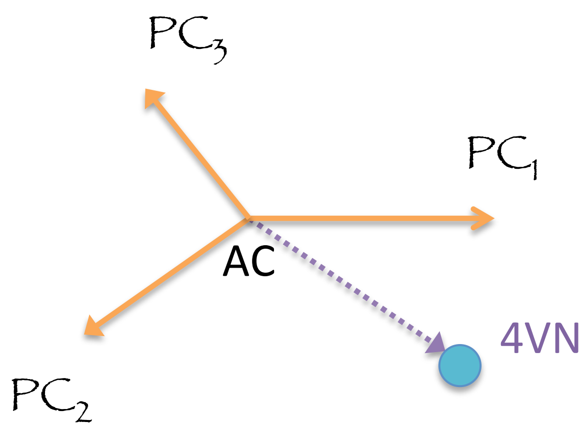

Minor correction are made by local search process.

EPCA demo

Physical vector space

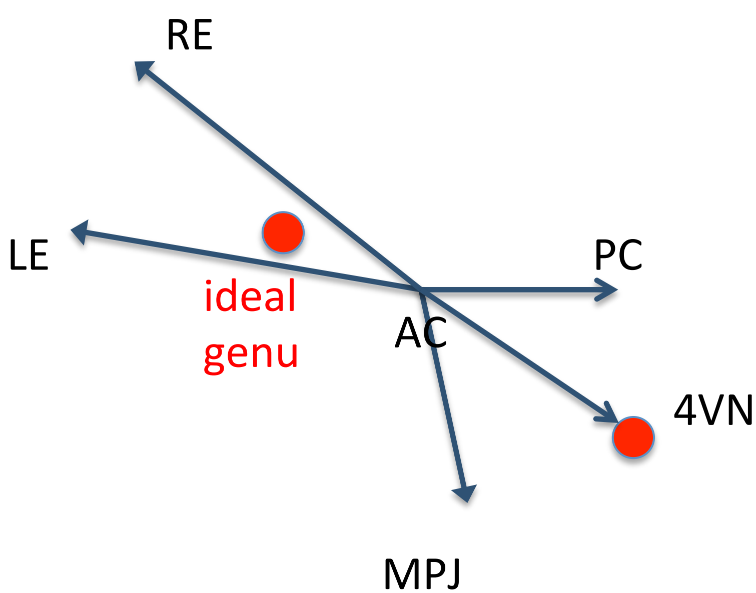

Revolutionarily/iteratively add newly estimated landmarks vector (e.g. 4VN) to the physical vector space.

Other new landmarks such as genu can be estimated in a similar way but with additional information from previously estimated landmarks (e.g. 4VN).

Local search estimation

Local search using statistical shape models

- Template matching: dot product
- Reduce anisotropic error: ten uniformly-rotated copies
- Shape: Cylinder $V = \pi \times R^2 \times h$
- Size (*mm*): R = 5, h = 10 (salient – precise anatomical definition)
  R = 8, h = 16 (quasi – regional extrema)

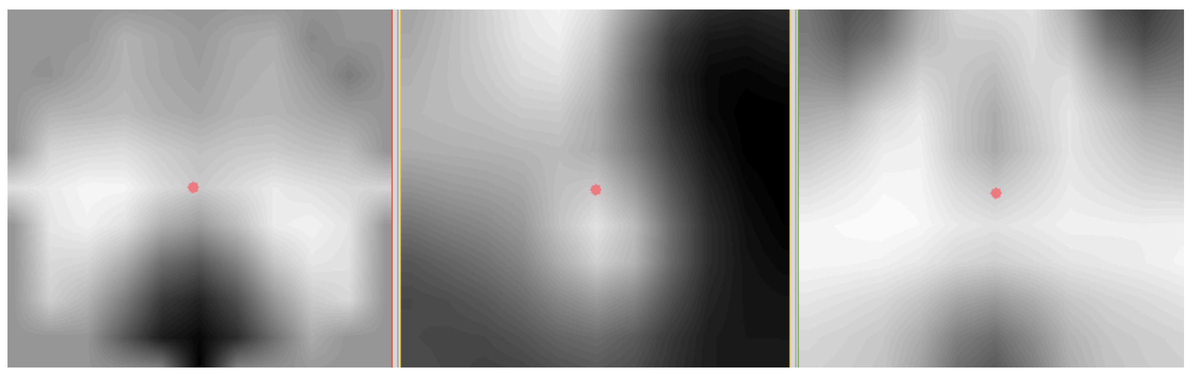

Example: Center slices of a T_1-weighted AC template

Local search using statistical shape models

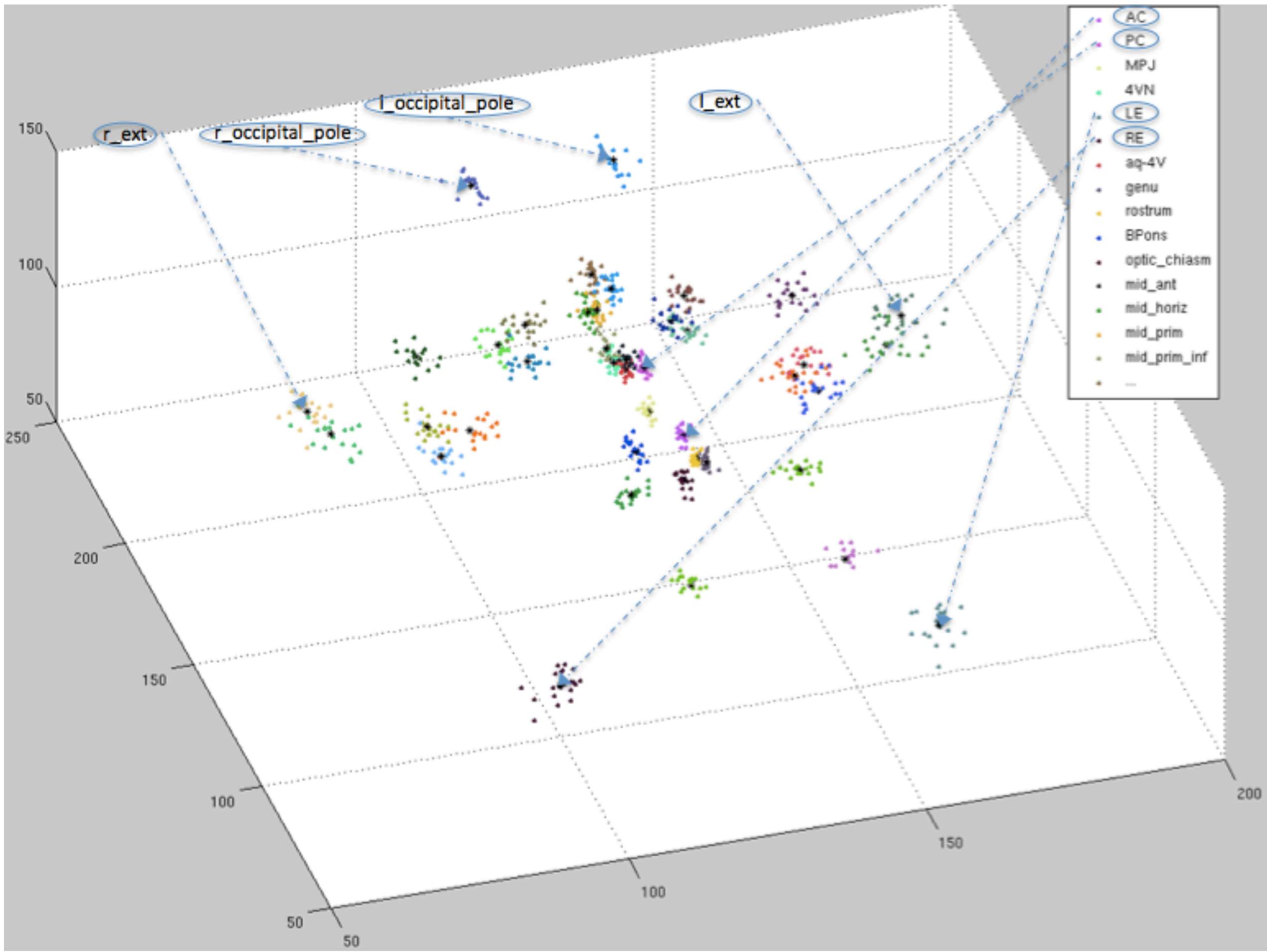

Constellation distribution

The University of Iowa College of Engineering

Local search using statistical shape models

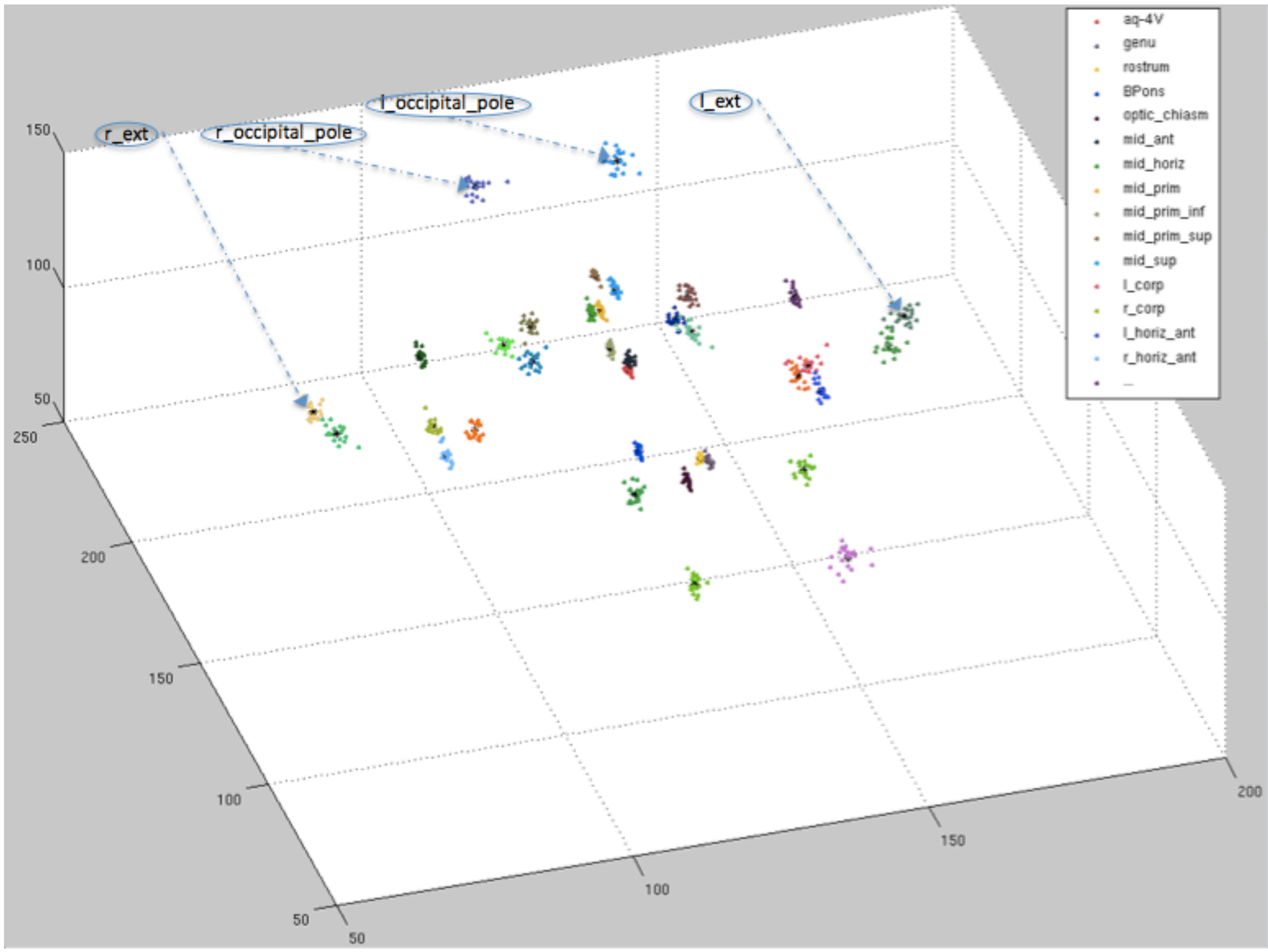

Error residuals using LME-EPCA

Local search using statistical shape models

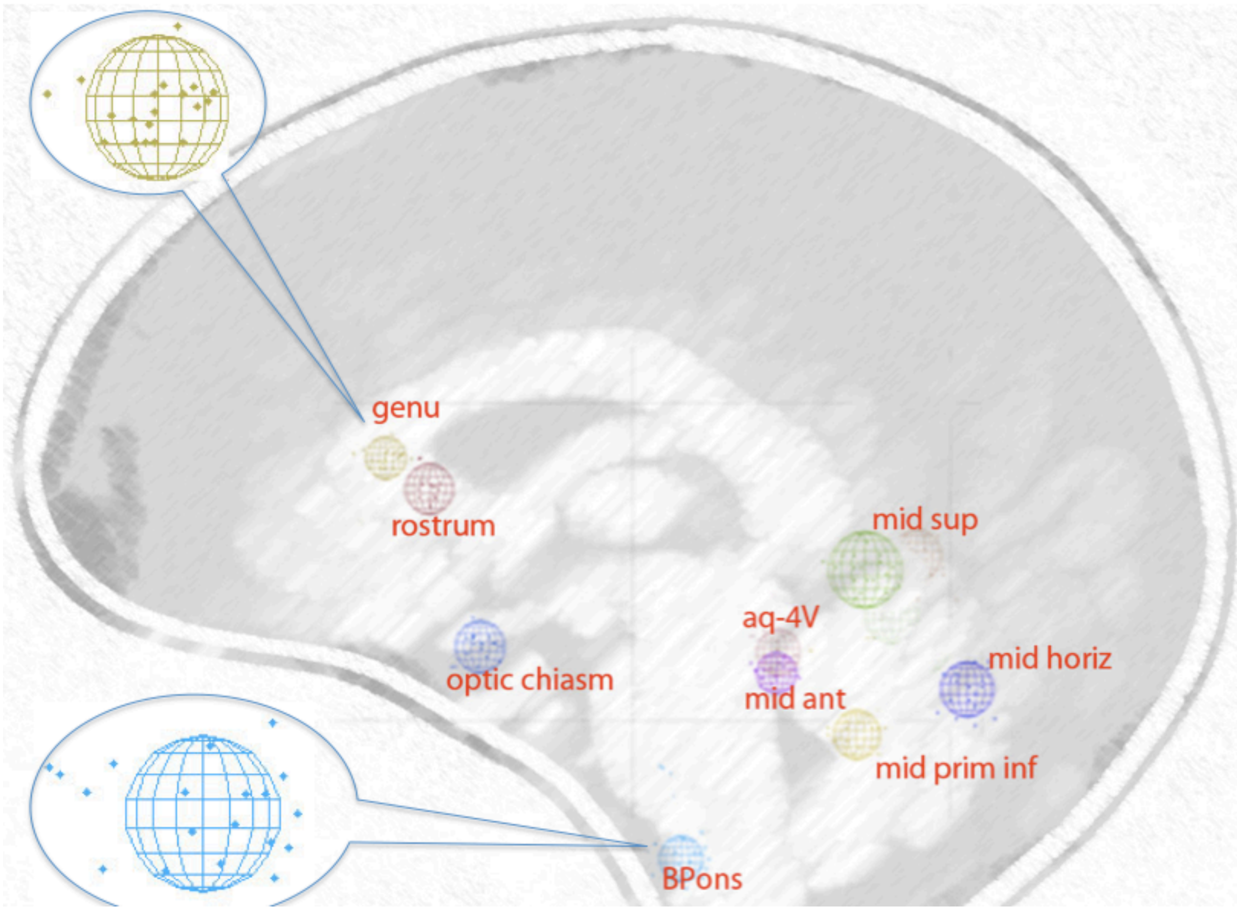

Constellation distribution in sagittal view

Local search using statistical shape models

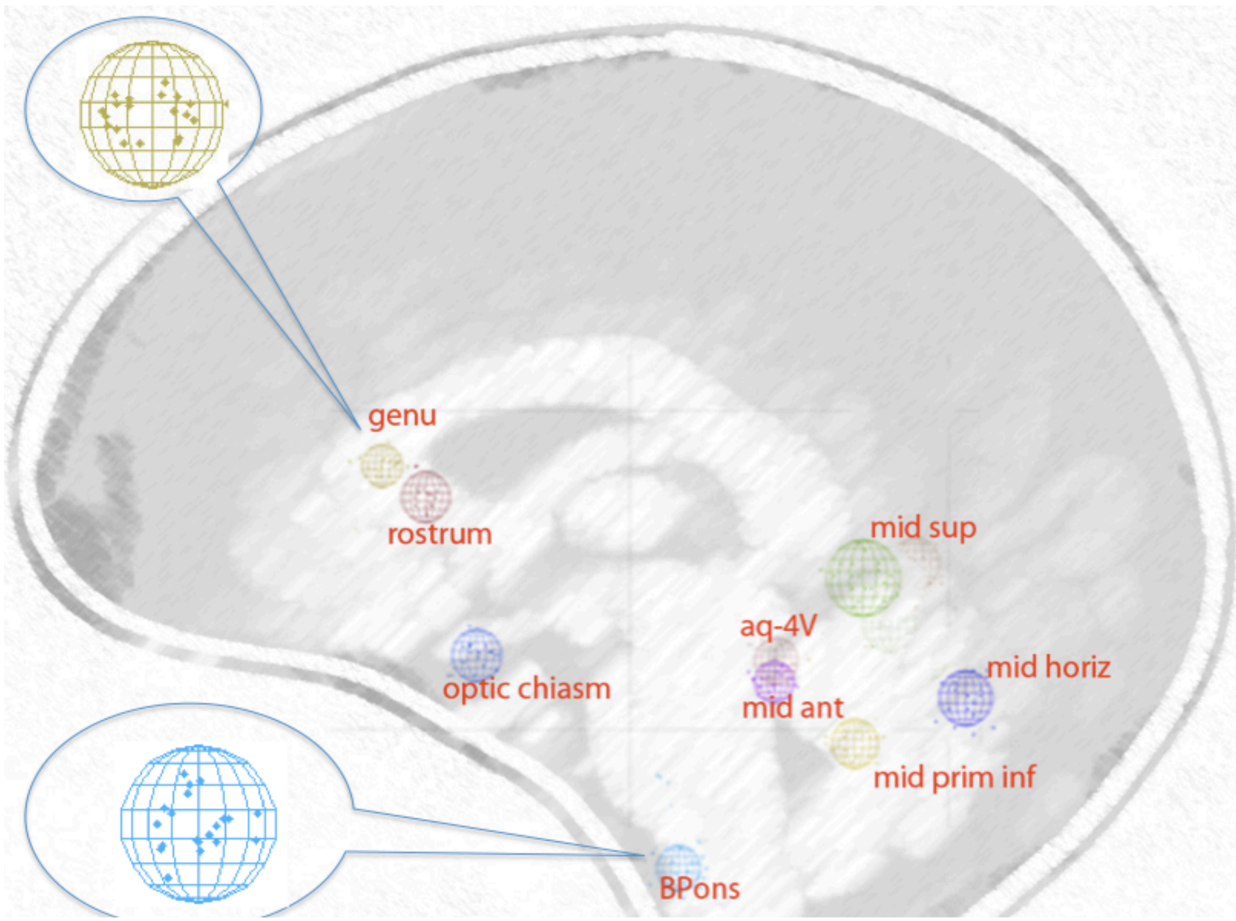

Error residuals using LME-EPCA in sagittal view

Detection process review

Detection process demo

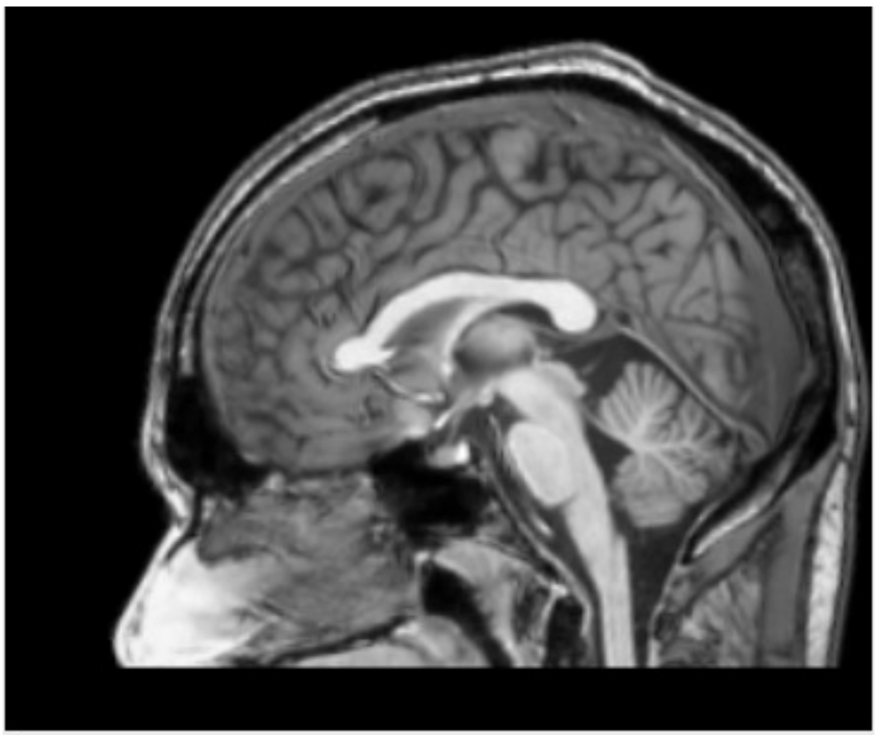

The input image

Detection process demo

Precondition: none
CM by Otsu thresholding and a top-down maximum sphere radius estimation (CM is used as a reference point to find MPJ when relatively few information is obtained)

Detection process demo

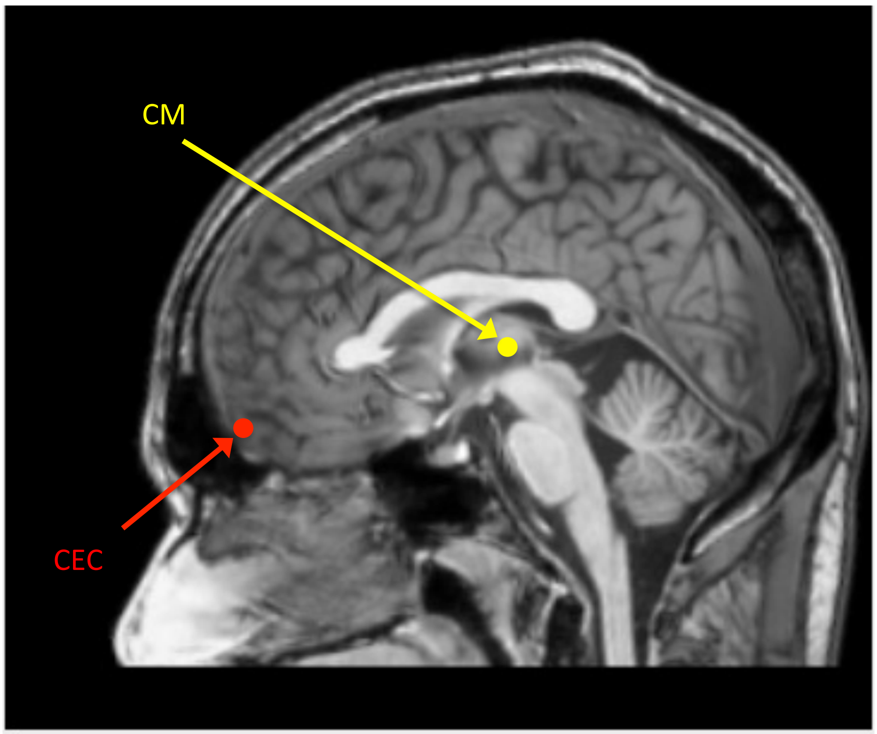

Precondition: LE and RE are reasonably found by the radial Hough transform

Center of eye centers (**CEC**) is used as a reference point to guide the search when there is some rotation along L-axis in a LPS coordinate system.

Detection process demo

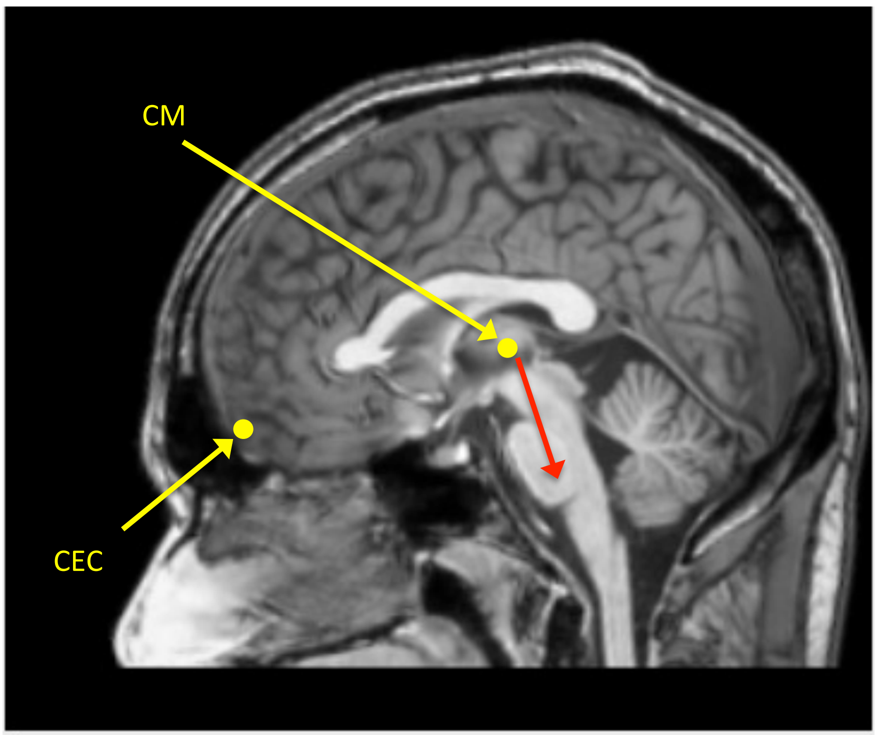

Precondition: CM is correct
MPJ by a correlation based local search which is centered at CM plus average CM-to-MPJ vector from statistical shape model (SSM)

Detection process demo

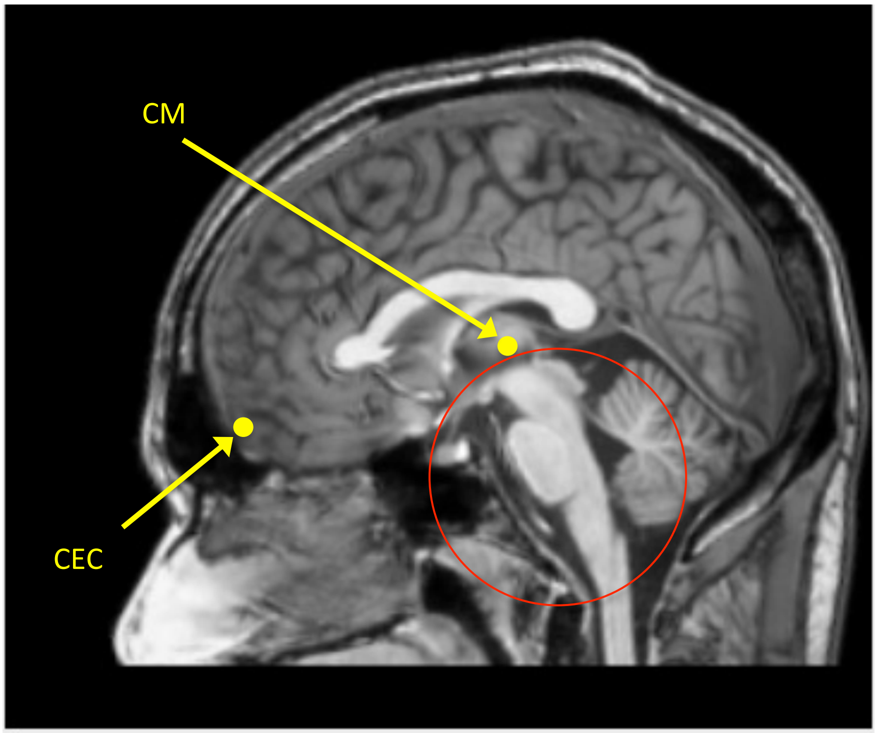

Precondition: CM is correct
MPJ by a correlation based local search which is centered at CM plus average CM-to-MPJ vector from statistical shape model (SSM)

Detection process demo

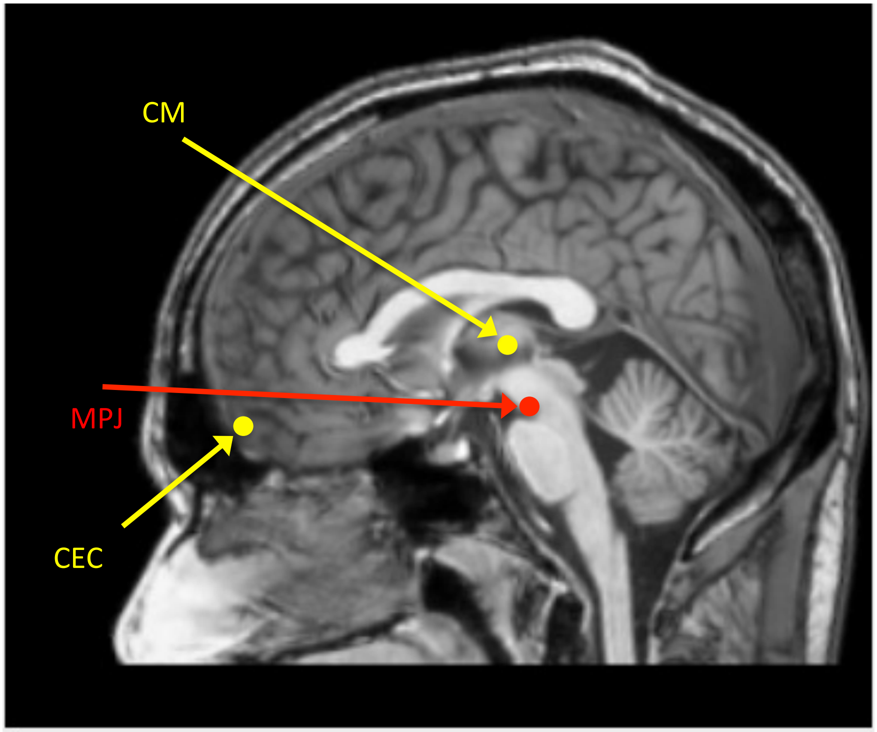

Precondition: CM is correct
MPJ by a correlation based local search which is centered at CM plus average CM-to-MPJ vector from statistical shape model (SSM)

Detection process demo

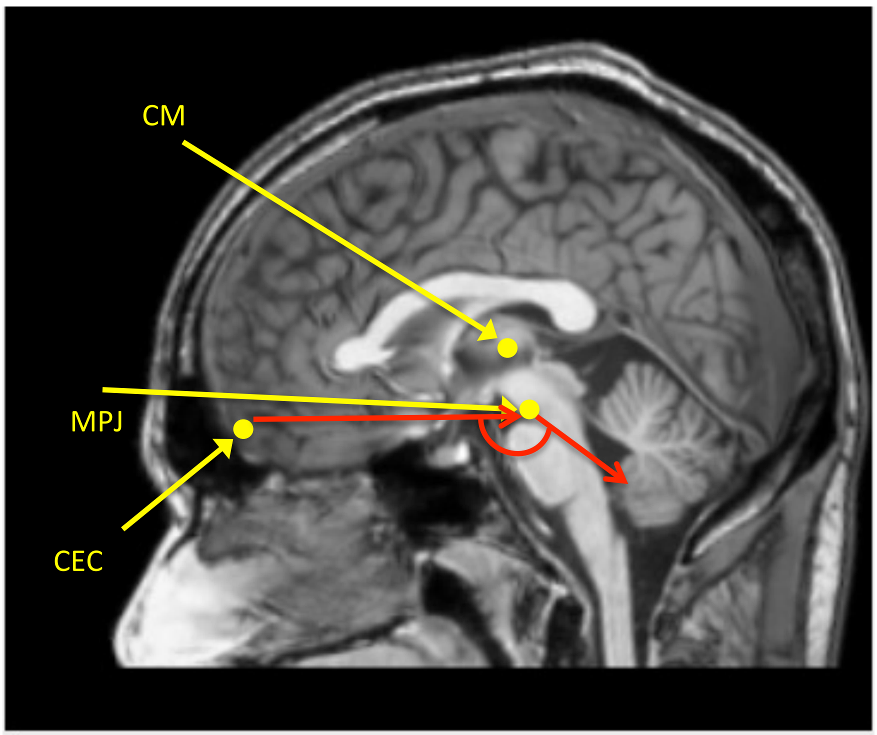

Precondition: the estimated CEC and MPJ are reasonable

The estimation of **4VN** starts with the morphometric constraints among CEC, MPJ, and 4VN

Detection process demo

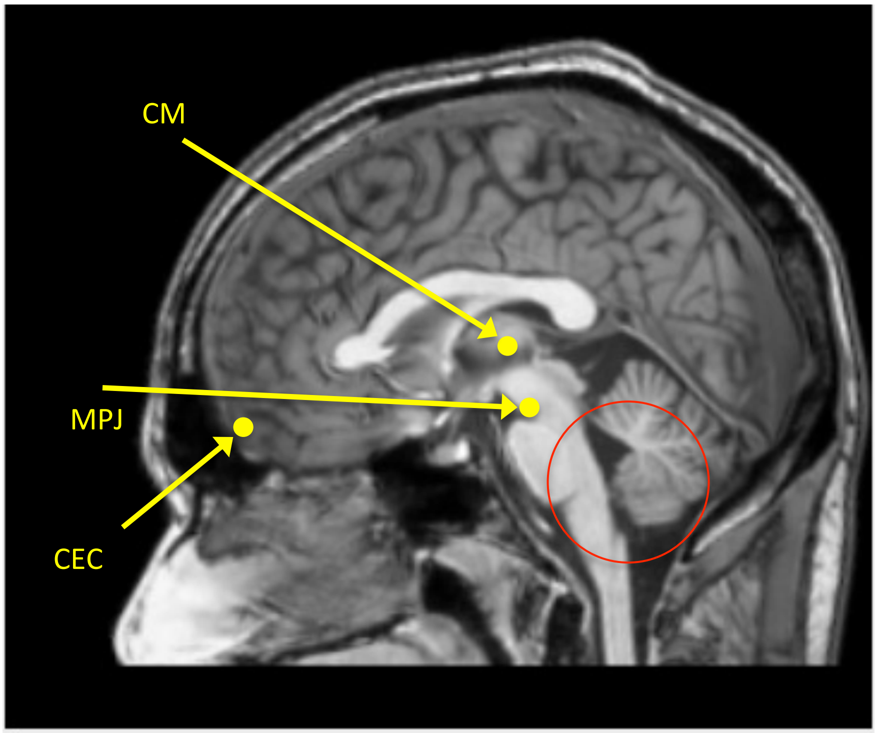

Precondition: the estimated CEC and MPJ are reasonable
The estimation of **4VN** starts with the morphometric constraints among CEC, MPJ, and 4VN

Detection process demo

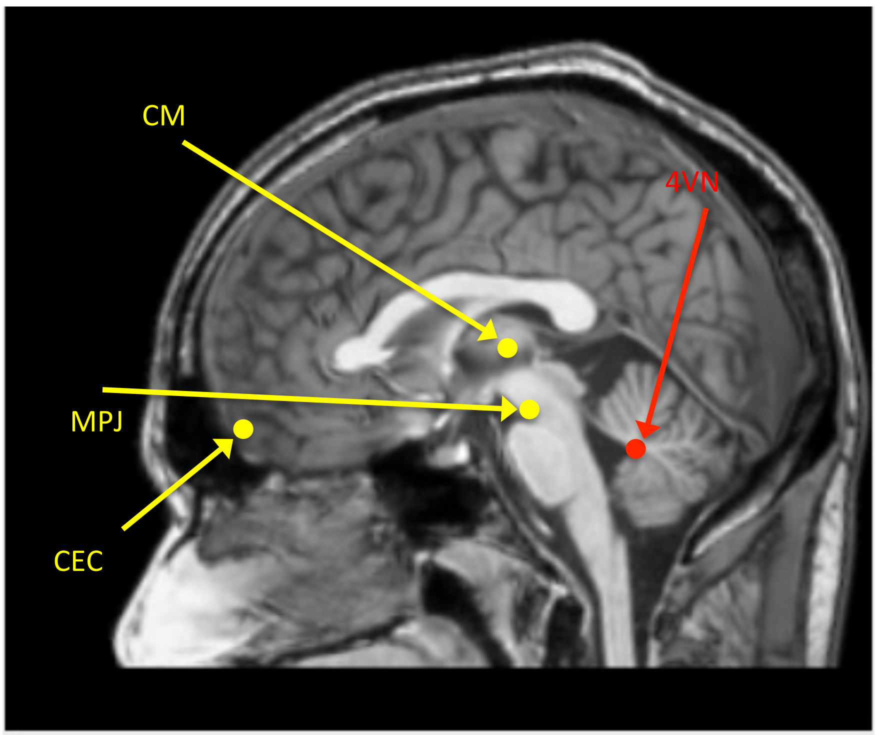

Precondition: the estimated CEC and MPJ are reasonable
The estimation of **4VN** starts with the morphometric constraints among CEC, MPJ, and 4VN.
A local search is performed near the search center.

Detection process demo

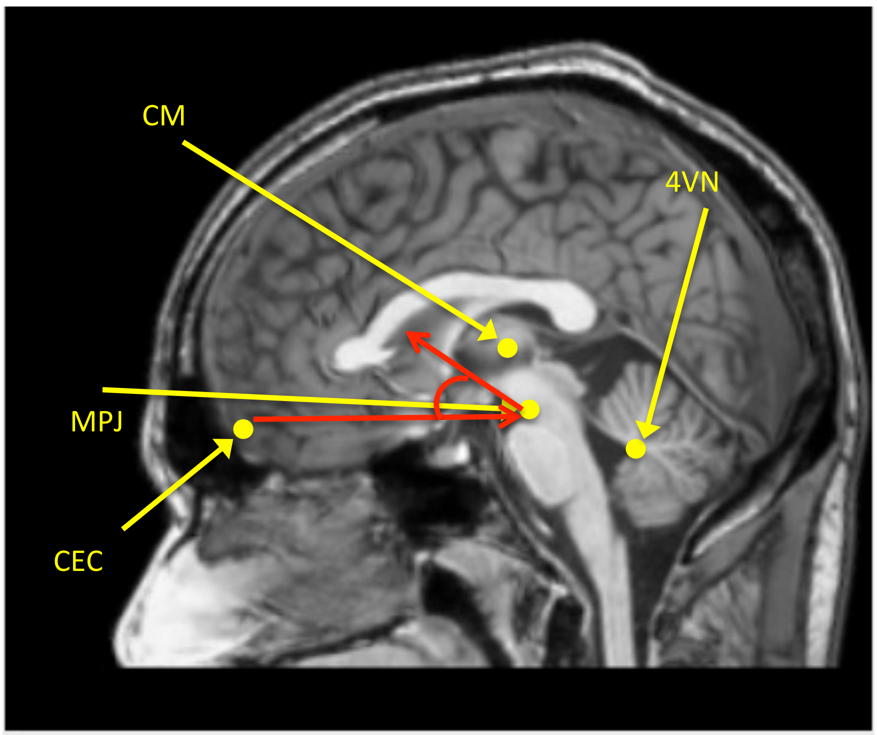

Precondition: the estimated CEC and MPJ are reasonable
The estimation of **AC** starts with the morphometric constraints among CEC, MPJ, and AC.
A local search is performed near the search center.

Detection process demo

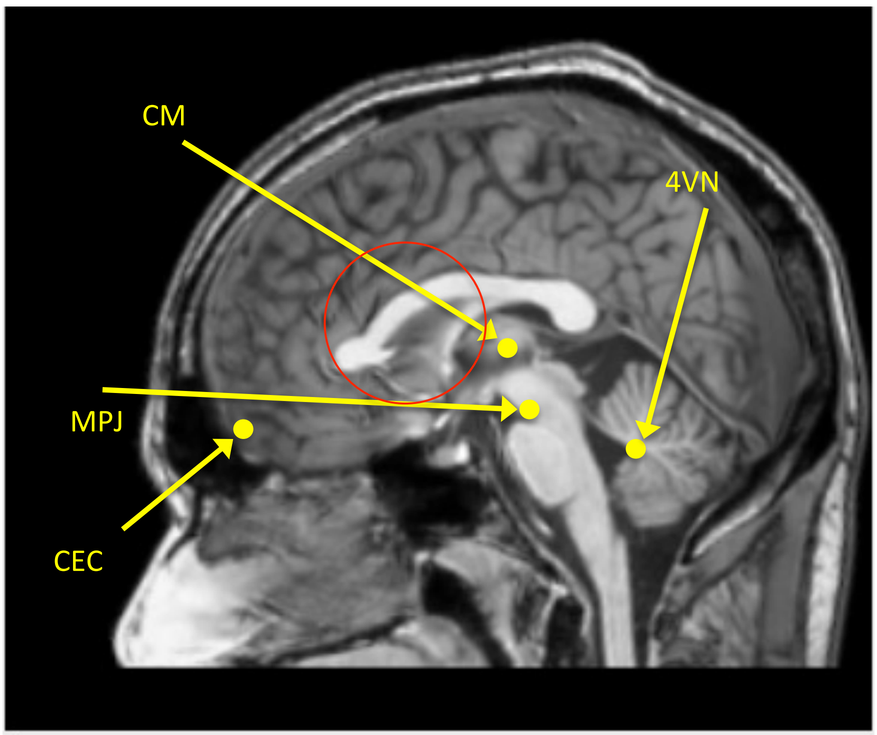

Precondition: the estimated CEC and MPJ are reasonable
The estimation of **AC** starts with the morphometric constraints among CEC, MPJ, and AC.
A local search is performed near the search center.

Detection process demo

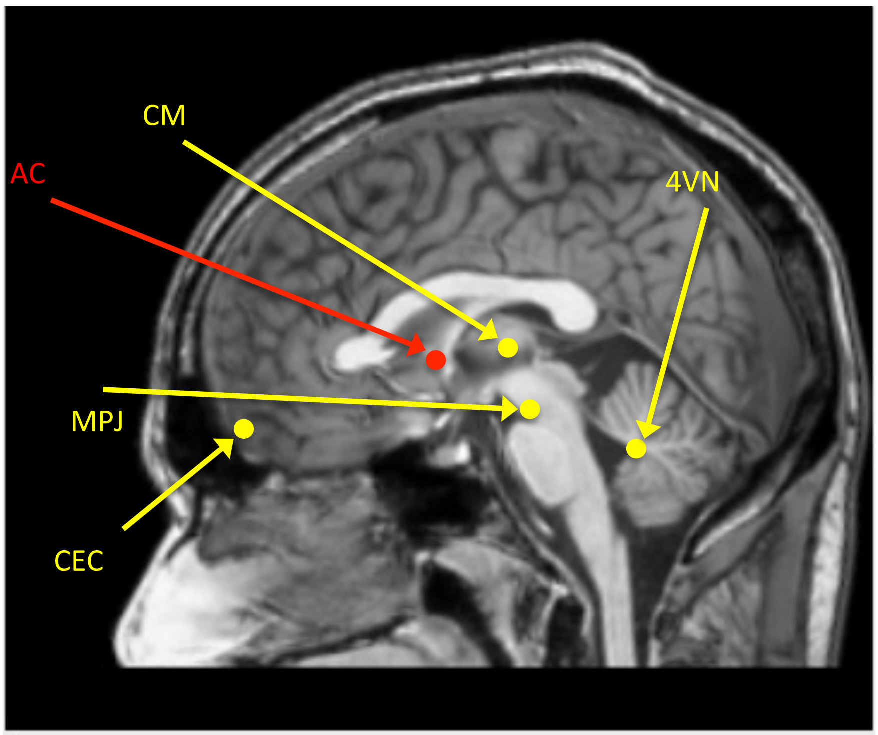

Precondition: the estimated CEC and MPJ are reasonable
The estimation of **AC** starts with the morphometric constraints among CEC, MPJ, and AC.
A local search is performed near the search center.

Detection process demo

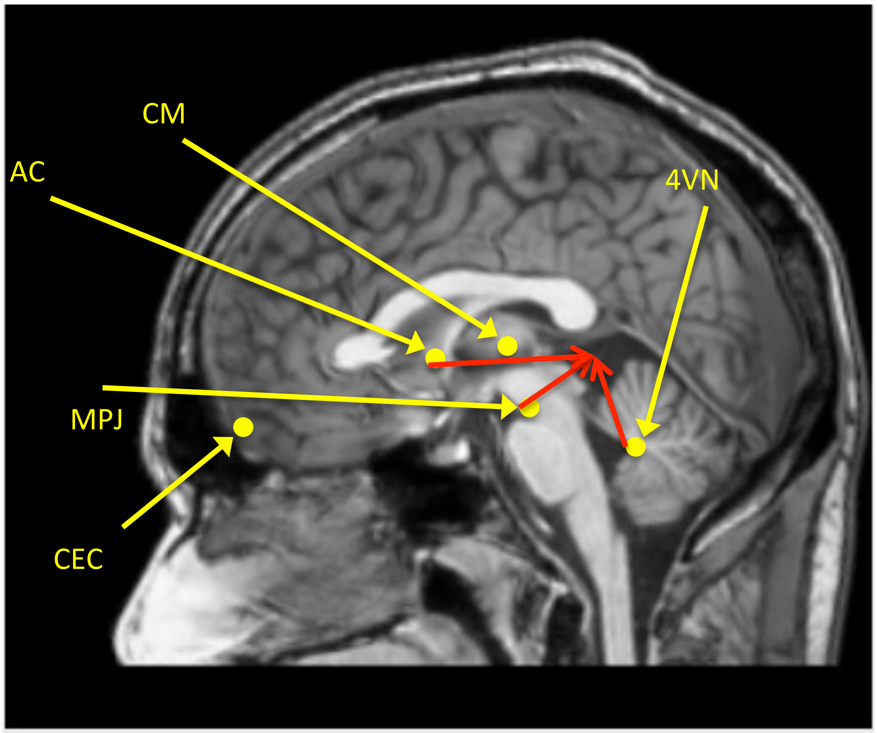

Precondition: the estimated AC, MPJ, and 4VN are reasonable
PC is estimated by a linear model among landmarks

Detection process demo

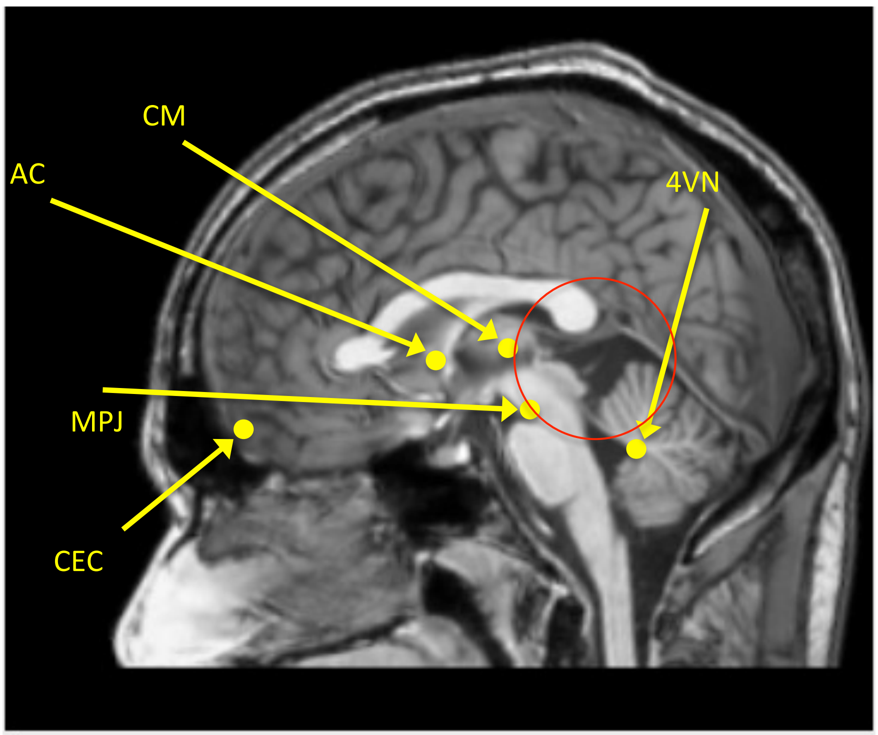

Precondition: the estimated AC, MPJ, and 4VN are reasonable
PC is estimated by a linear model among landmarks

Detection process demo

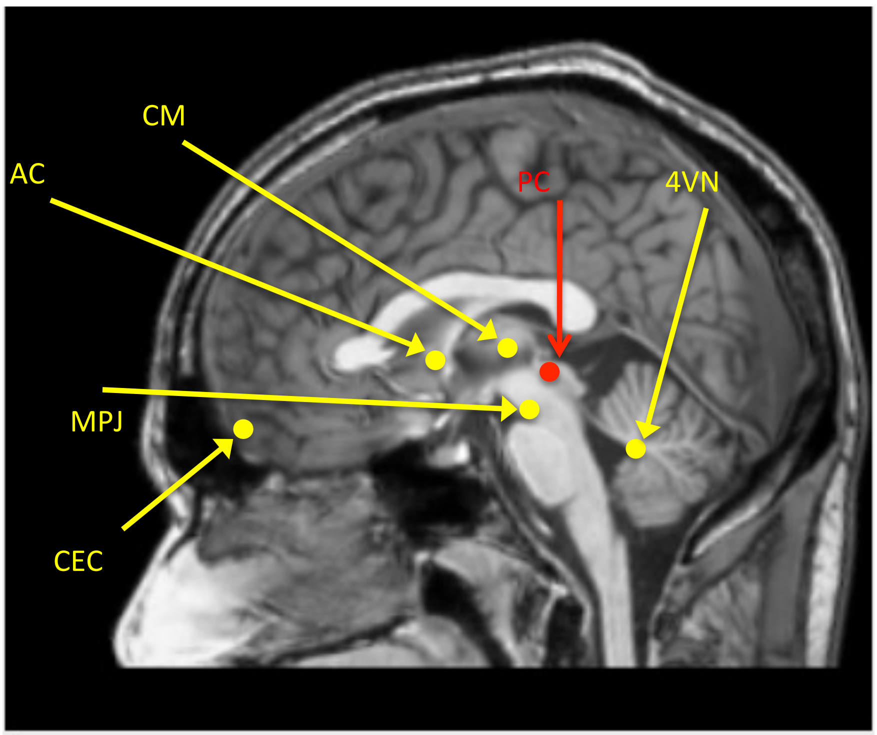

Precondition: the estimated AC, MPJ, and 4VN are reasonable
PC is estimated by a linear model among landmarks

Detection process demo

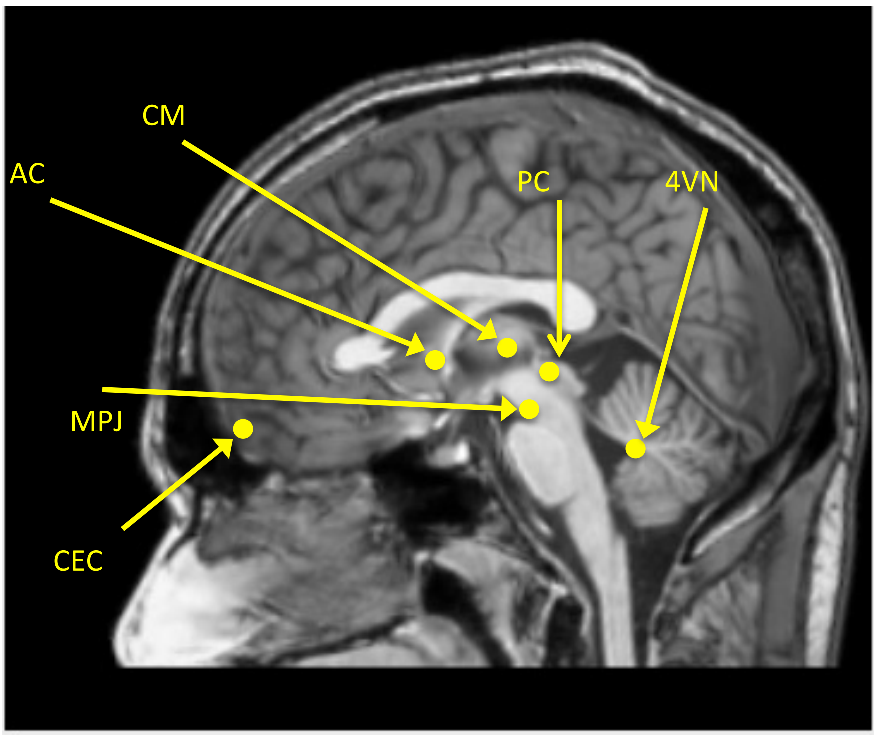

Other landmarks are estimated in a way similar to what we have demonstrated in “EPCA demo”

Result

Constellation detection result

Average detection errors in *mm*

		T_1 Images		T_2 Images	
	Landmark Name	**Mean**	**Std**	**Mean**	**Std**
Base	*ac*	0.97	0.14	1.11	0.54
	pc	1.05	0.76	1.51	0.80
	MPJ	0.78	0.47	0.85	0.33
	4VN	0.96	0.33	1.34	0.48
Midbrain	*aq-4V*	1.20	0.43	1.16	0.36
	genu	2.64	2.36	3.18	2.20
	rostrum	2.47	1.57	2.25	1.49
	BPons	1.89	1.20	2.02	0.89
	optic_chiasm	2.72	2.15	2.79	1.61
Off-midbrain	*l_ventricular_head*	4.10	3.99	4.38	3.04
	r_ventricular_head	2.80	1.68	3.69	2.03
	l_corp	5.73	5.39	6.65	4.09
	r_corp	3.68	3.55	4.96	3.56
	l_horiz_ant	6.83	5.60	8.80	4.82
	r_horiz_ant	7.12	4.95	7.83	4.82
	l_sup	8.06	3.77	8.14	4.66
	r_sup	6.71	4.40	7.32	4.59

Validation for landmark detection accuracy

10 training datasets
10 test datasets

Constellation detection result

Average detection errors in %

Name	mean	std
aq-4V	0.38	0.57
genu	0.30	0.04
rostrum	0.36	0.23
BPons	0.42	0.17
optic_chiasm	0.09	-0.48

(a) Improvement made by local search (in %) for several midbrain landmarks in T_1 images

Name	mean	std
l_ventricular_head	0.27	-0.16
r_ventricular_head	0.33	0.08
l_corp	0.19	-0.74
r_corp	0.35	-0.16
l_horiz_ant	0.21	-0.51
r_horiz_ant	0.06	-0.30
l_sup	0.05	-0.07
r_sup	0.01	-0.02

(b) Improvement made by local search (in %) for several off-midbrain landmarks in T_1 images

Validation for landmark detection accuracy

10 training datasets
10 test datasets

Constellation detection result

Average detection errors in *mm*

Name	L	P	S
ac	0.48	0.53	0.45
pc	0.42	1.47	0.62
$4VN$	0.61	0.73	0.93

(a) T_1 peg_MR datasets (215 subjects)

Name	L	P	S
ac	0.46	0.73	0.50
pc	0.34	1.02	1.14
$4VN$	0.50	0.89	0.95

(b) T_1 AV_MR datasets (98 subjects)

Validation for landmark detection accuracy

20 training datasets

Inconsistency in human placement of landmarks

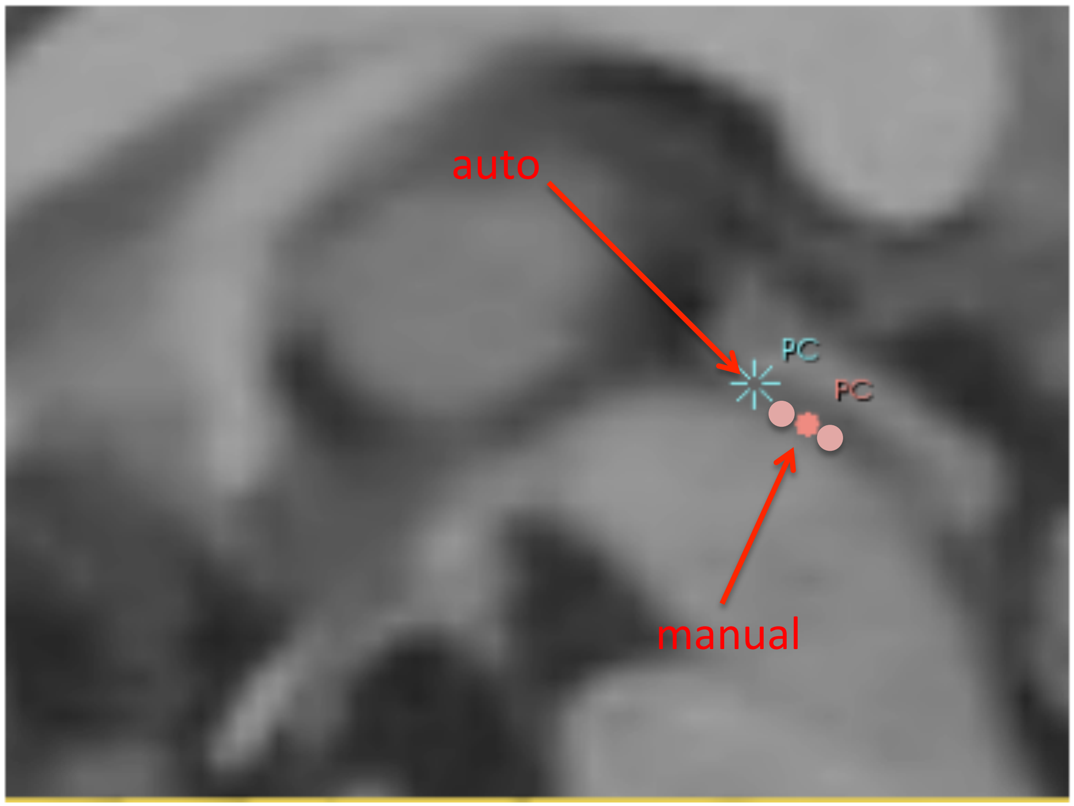

Validation for landmark detection reliability

20 training datasets

35% error > 2 *mm*

Atlas construction result

Moving image with fixed landmarks

Fixed image with fixed landmarks

Warped image with fixed landmarks

TPS warping result

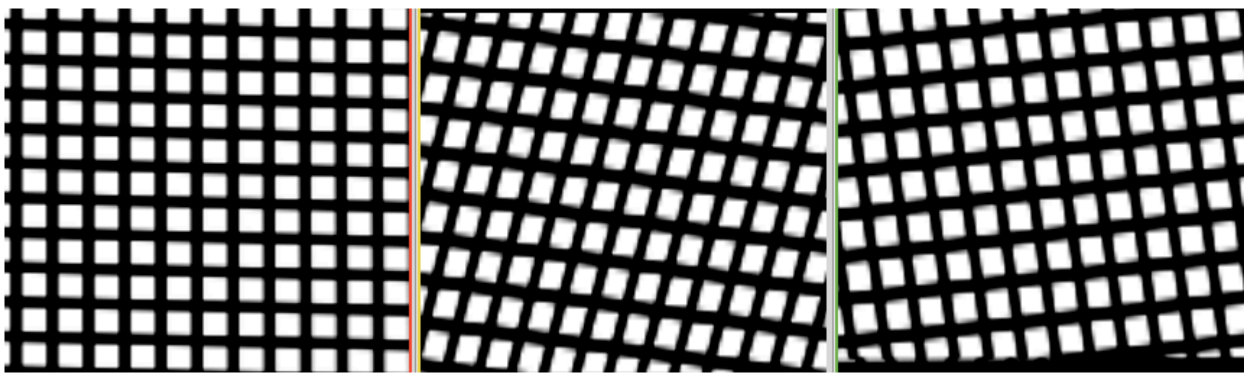

L

P

S

Deformation field

Atlas construction result

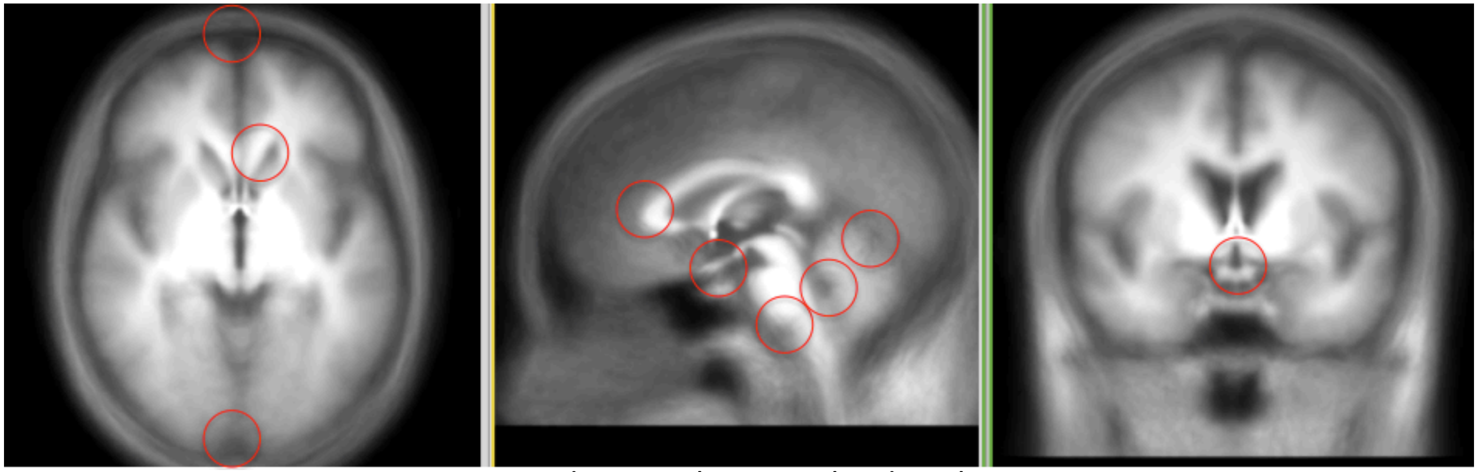

Rigid, 206 subjects, 3 landmarks

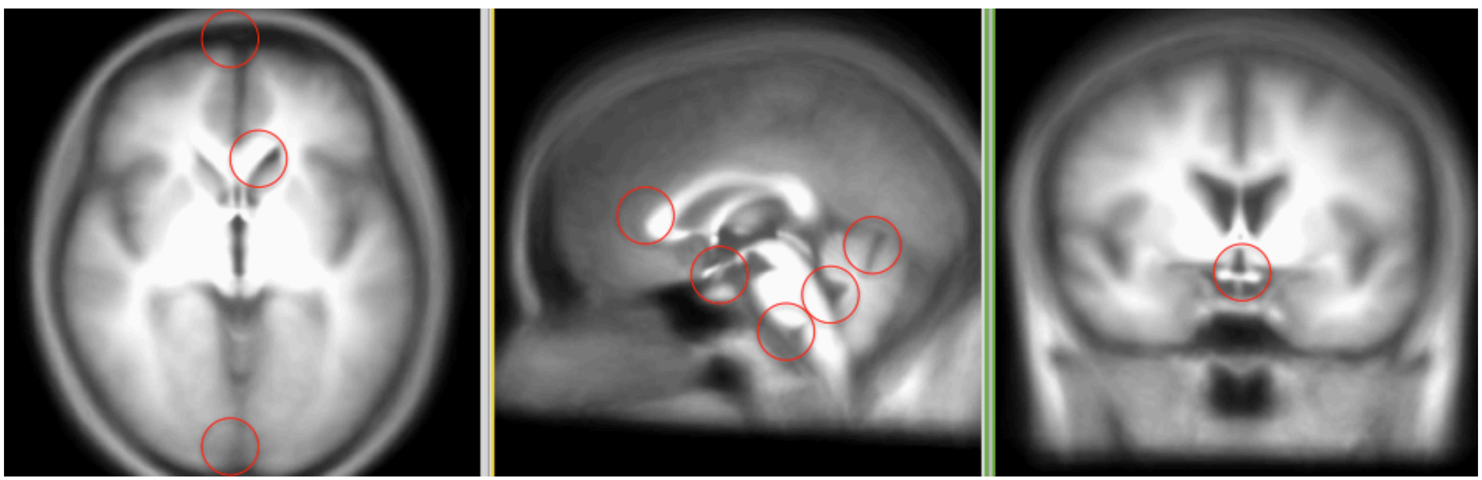

TPS, 206 subjects, 41 landmarks

Atlas construction result

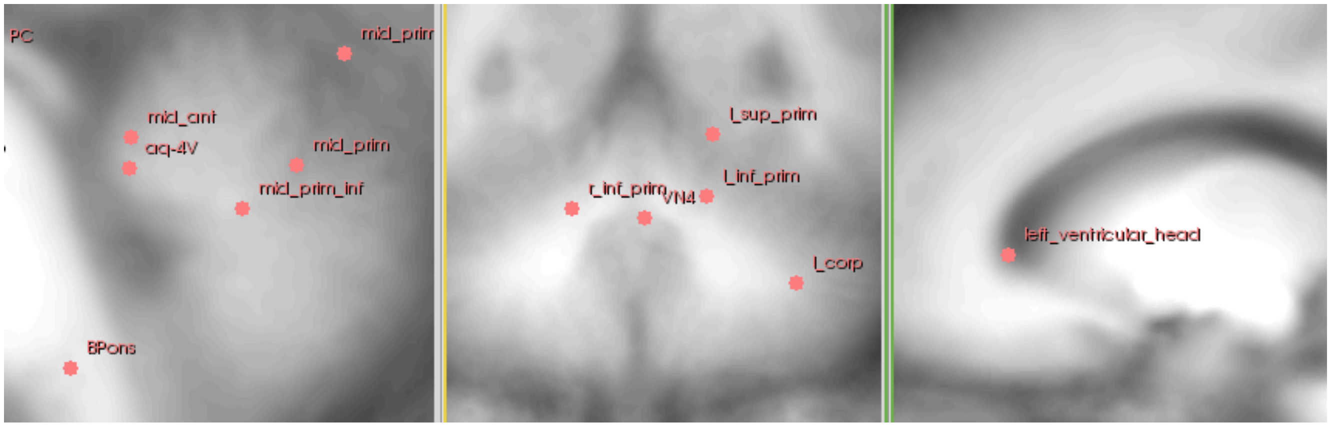

Rigid, 206 subjects, 3 landmarks

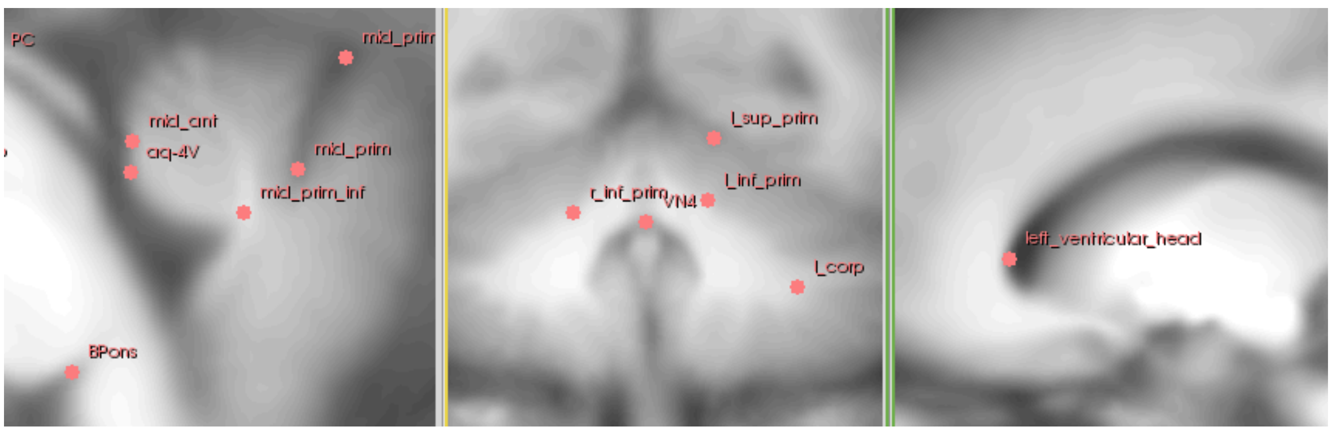

TPS, 206 subjects, 41 landmarks

Notice the regions near 4th ventricle, primary fissure, ventricular head, etc

Atlas construction result

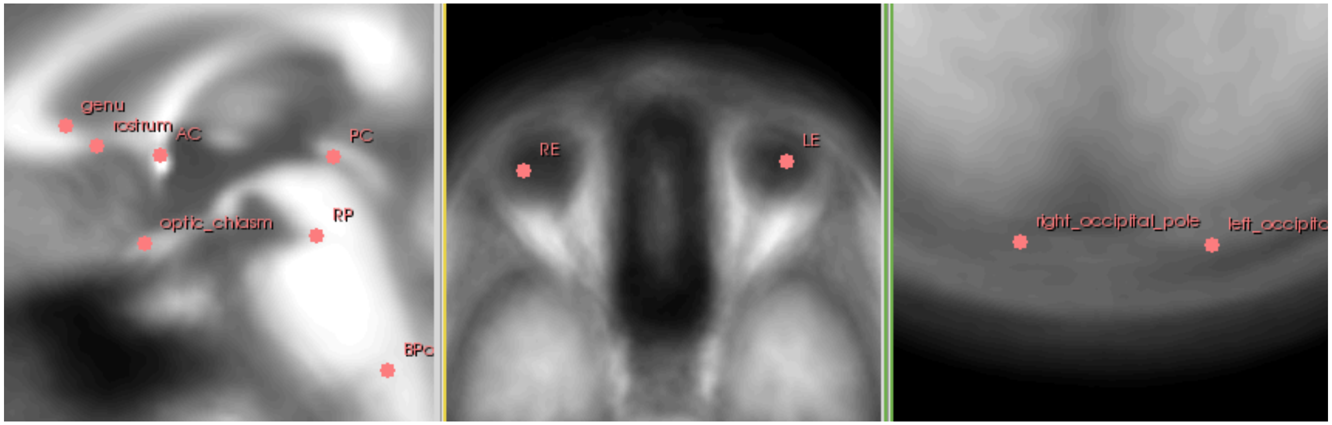

Rigid, 206 subjects, 3 landmarks

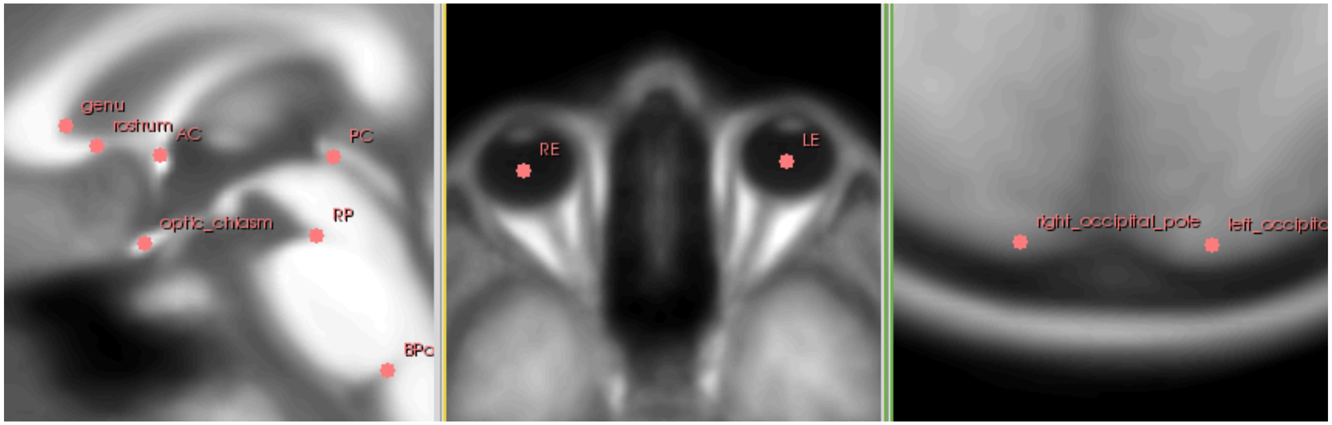

TPS, 206 subjects, 41 landmarks

Notice the regions genu, rostrum, optic chiasm, basal pons, cornea, boundary between brains and skull, etc

The University of Iowa
College of Engineering

Conclusion

- This work explored one automated, consistent, and efficient way of estimating landmark constellation by
  - landmark morphometrics + image intensity
  - Principal components + statistical shape models

Conclusion

The proposed method is

- Accurate (salient landmarks)
- Scalable (by EPCA)
- Generalizable
  - Different modalities
  - Different anatomical regions (EPCA algorithm)
- Robust
  - Orientation
  - Spacing
  - Origin

- Thank you!
- Questions?